AFRL-AFOSR-JP-TR-2019-0048

A Study of Material and Optical Properties of Nano Diamond Wires

Nong-Moon Hwang
SEOUL NATIONAL UNIVERSITY
SNUR&DB FOUNDATION RESEARCH PARK CENTER
SEOUL, 151742
KR

07/29/2019
Final Report

Air Force Research Laboratory
Air Force Office of Scientific Research
Asian Office of Aerospace Research and Development
Unit 45002, APO AP 96338-5002

REPORT DOCUMENTATION PAGE

Form Approved
OMB No. 0704-0188

1. REPORT DATE *(DD-MM-YYYY)*	2. REPORT TYPE	3. DATES COVERED *(From - To)*
29-07-2019	Final	22 Sep 2015 to 21 Sep 2018

4. TITLE AND SUBTITLE
A Study of Material and Optical Properties of Nano Diamond Wires

5a. CONTRACT NUMBER

5b. GRANT NUMBER
FA2386-15-1-4067

5c. PROGRAM ELEMENT NUMBER
61102F

6. AUTHOR(S)
Nong-Moon Hwang, Jimmy Xu

5d. PROJECT NUMBER

5e. TASK NUMBER

5f. WORK UNIT NUMBER

7. PERFORMING ORGANIZATION NAME(S) AND ADDRESS(ES)
SEOUL NATIONAL UNIVERSITY
SNUR&DB FOUNDATION RESEARCH PARK CENTER
SEOUL, 151742 KR

8. PERFORMING ORGANIZATION REPORT NUMBER

9. SPONSORING/MONITORING AGENCY NAME(S) AND ADDRESS(ES)
AOARD
UNIT 45002
APO AP 96338-5002

10. SPONSOR/MONITOR'S ACRONYM(S)
AFRL/AFOSR IOA

11. SPONSOR/MONITOR'S REPORT NUMBER(S)
AFRL-AFOSR-JP-TR-2019-0048

12. DISTRIBUTION/AVAILABILITY STATEMENT
A DISTRIBUTION UNLIMITED: PB Public Release

13. SUPPLEMENTARY NOTES

14. ABSTRACT
The Seoul National University (SNU) group succeeded to capture the nanodiamonds which were generated at the gas phase. The nanoparticles based on the TCN (Theory of charged nanoparticle) will lead to a new approach in the SiV nanodiamond area. The SNU group came to understand the existence of various allotropes of nanodiamond and their formation in relation with experimental conditions. This understanding will help in synthesizing the SiV cubic-nanodiamonds in HFCVD.

15. SUBJECT TERMS
diamond, nanowire, cyrstal, nanoparticles, carbon

16. SECURITY CLASSIFICATION OF:			17. LIMITATION OF ABSTRACT	18. NUMBER OF PAGES	19a. NAME OF RESPONSIBLE PERSON
a. REPORT	b. ABSTRACT	c. THIS PAGE			KNOPP, JEREMY
Unclassified	Unclassified	Unclassified	SAR		19b. TELEPHONE NUMBER *(Include area code)* 315-227-7006

Standard Form 298 (Rev. 8/98)
Prescribed by ANSI Std. Z39.18

AOARD Final Tech Report

Title: A Study of Material and Optical Properties of Nano Diamond Wires

Principle Investigator:

N.M. Hwang, Professor of Materials Science and Engineering, Seoul National University, Korea
Tel: +82-2-880-8922
E-mail: nmhwang@snu.ac.kr

Co-PI: Jimmy Xu, WCU Professor of Hybrid Materials, Department of Materials Science and Engineering, Seoul National University, Korea & Professor of Engineering and Professor of Physics, Brown University, United States
Tel: +1-401-863-1439
E-mail: jimmy_xu@brown.edu

Contract Number: FA2386-15-1-4067

AOARD Case Number: 15IOA067

AOARD Program Manager: Seng Hong, Ph.D.
Tel: +81-3-6385-3377
E-mail: seng.hong@us.af.mil

Period of Performance: 3 years (Sept 22, 2015 – Dec 20, 2018)

Submission Date: Dec 20, 2018

A Study of Material and Optical Properties of Nano Diamond Wires

N.M. Hwang
Professor of Materials Science and Engineering, Seoul National University, Korea

Jimmy Xu
WCU Professor, Department of Materials Science and Engineering, Seoul National University, Korea &
Professor of Engineering and Physics, Brown University, United States

Abstract

This Korea-USA collaborative project, sponsored by AOARD for 3 years (July 18th, 2015 - April 17th, 2018), "A study of material and optical properties of nano diamond wires (15IOA067)", aspired to find a way to synthesize a new form of carbon, crystalline diamond nanowires and SiV diamond nanoparticle, and then to characterize them for device applications in nanophotonics, nanoelectronics, and quantum information processing. Reproducible synthesis of the crystalline diamond nanowires has proven to be extraordinarily challenging, to us as well as to the field in general. Our lab has so far had the only reported success. However, if a method is successfully developed with reproducibility, it would bring yet another new member into the family of carbon allotropes, this time on the sp^3 side. It would also generate new insights into the phases, stability, and functionalization of diamond altered under nanoscale confinement, and pave way for a broad range of applications in nanoelectronics and nanophotonics, e.g., quantum information processing.
Enabled by the AOARD support, the Korean-US collaborative team has taken on this challenge to investigate the feasibility of reproducible growth of diamond nanowires and tried to synthesize the SiV cubic nanodiamond during the period of performance. The SNU group succeeded to capture the nanodiamonds which were generated at the gas phase. The nanoparticles based on the TCN (Theory of charged nanoparticle) will lead to a new approach in the SiV nanodiamond area. The SNU group came to understand the existence of various allotropes of nanodiamond and their formation in relation with experimental conditions. This understanding would be a great help in synthesizing the SiV cubic-nanodiamonds in HFCVD. The Brown team, led by Co-PI Professor Jimmy Xu and Dr. Do-Joong Lee, has supported the SNU group for establishing reproducible growth of diamond and other crystalline carbon wires. Various efforts have been made, including the catalyst-engineering for formation of ultrathin metal nanoparticles and the introduction of diamond or graphitic seed layers. In addition, a new fabrication concept of porous Si has suggested for a potential realization of Si-based single photon sources.

1. Introduction

This Korea-USA collaborative project, sponsored by AOARD, "A study of material and optical properties of nano diamond wires (15IOA067)", aspired to find a way to synthesize a new form of carbons, such as crystalline diamond/graphite nanowires and diamond nanoparticles doped with silicon vacancy, and then to characterize them for device applications in nanophotonics, nanoelectronics, and quantum information processing. Diamond nanoparticles doped with silicon vacancy have been known for single photon emitter. The Professor Hwang's lab in Seoul National University (SNU) had produced the impressive results for producing high-quality diamond nanoparticles in Year-1. Specifically, Dr. Jin woo Park, who led the project in the SNU side, had a great success on capturing nanodiamonds which were generated in a gas phase. In addition, the Hwang's group had tried to solve the curious phenomena related to the captured diamond nanoparticles. According to the "Theory of Charged Nanoparticles (TCN), Diamond nanoparticles had various characteristics and those physical and chemical properties

could affect synthesizing the nanodiamond doped with silicon vacancy for single photon emission.

The SNU group, led by Professor Nong-Moon Hwang, has championed for the development of a new comprehensive theory on the growth mechanism in various CVD systems, named as "Theory of Charged Nanoparticles (TCN)". In Year-1, The SNU team had a success to capture the nanodiamond, and this remarkable progress toward the goal of the project made a possibility to synthesize the diamond nanoparticles doped with silicon vacancy. In Year-2, the SNU team worked on the synthesis of diamond nanoparticles reproducibly and tried to solve the interesting phenomena about the diamond nanoparticles generated in gas phase. In Year-3, most of efforts have been made to understand the crystal structure of nanodiamonds captured under various experimental conditions.

Among various phenomena observed during this study, one of the problems was that nanodiamonds captured at 600 ^{o}C have d-spacing of 1.8 Å, which is not expected in the cubic diamond. Finally, the SNU team found out that nanodiamonds with 1.8 Å d-spacing are rather close to a lonsdaleite diamond which has a hexagonal structure. The SNU team has continued to capture nanodiamonds at various temperatures of graphitic flake membranes, which were thick enough to survive even under severely damaging conditions of high filament temperature and etching by atomic hydrogen. Under such conditions SiO and carbon membranes were so severely damaged that nanodiamonds could not be captured. The effect of methane concentration on the size and structure of captured nanodiamonds was also studied. The structure of nanodiamonds was analyzed with a focus on whether nanodiamonds had d-spacing values of cubic diamond. This is because only cubic nanodiamond among many allotropes has a SiV center for single photon emission of high efficiency. The team also revealed that the surface condition of W filaments for electron emission has an effect not only on the size and structure of captured nanodiamonds but also on the quality and the growth rate of diamonds deposited on the substrate.

The SNU team has been supported by the Brown team, led by Co-PI Professor Jimmy Xu and Dr. Do-Joong Lee for establishing reproducible growth of diamond and other crystalline carbon nanowires. Under the support of AOARD, Brown team has given efforts on the front of the catalyst-engineered CVD approaches, such as the utilization of ultrasmall iron family or noble metals and the careful control and optimization of process parameters. By leveraging from these efforts, the team has continued and extended the approaches to introduce a new seed layer of diamond or graphitic carbon for the growth of diamond nanowires. Still the reproducible growth of the diamond nanowires and understanding of underlying growth mechanisms are greatly challenging, but the team has continued many growth trials and confirmed promising results to achieve the goals of this project in the near future. Finally, the efforts have been extended to develop a new concept of fabrication porous Si by a simple metal-assisted gas-phase etching (MAGPE). Beyond the period of this project, this porous Si is to be used for implanting color centers, such as Si-G centers, and to be tested as a potential Si-based single photon sources.

2. Results and Discussion

1) Gas phase generation of diamond nanoparticles

Hwang's group succeed to diamond nanoparticles in gas phase were nucleated in HFCVD. To confirm the generation of diamond nanoparticles in the gas phase under the synthesis condition of diamond films by HFCVD, the transmission electron microscope (TEM) grid membrane was exposed for 3-15 sec using a capturing apparatus and the grid membrane was observed by TEM. Two kinds of Cu mesh grids were used: one with a silicon monoxide membrane (Silicon Monoxide Type-A, TED PELLA, INC.) was for scanning TEM (STEM) imaging and the other with a carbon membrane (Ultrathin Carbon Type-A, TED PELLA, INC.) was for high resolution TEM (HRTEM). The Seoul Nat' team captured 30 mm below the hot filament and the temperature of substrate which was located in the capture zone was 600 ^{o}C. Since the membrane of the TEM Cu grid was so weak at temperature above 650 ^{o}C, the Seoul Nat' team tried to find the distance and that temperature. Although the capture

temperature is much less than the typical substrate temperature for the synthesis of diamond nanoparticles, which is normally higher than 900 °C, Dr. Jin-Woo Park, who is one of Hwang's group members, thought that these were a successful experiment condition for capturing diamond nanoparticles.

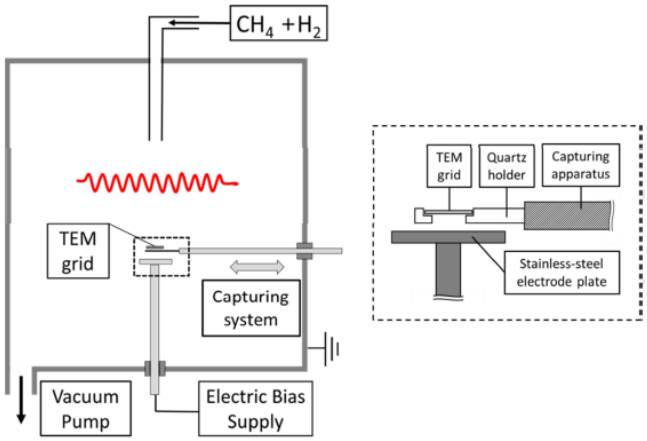

Fig. 1 Schematic of the experimental setup for capturing diamond nanoparticles generated in the gas phase of the HFCVD reactor. The capturing was done without or with the bias applied to the stainless-steel plate below the quartz holder of the TEM grid.

The Seoul Nat' team designed the capturing system for proving the gas-phase generation of diamond nanoparticles. And we succeeded in capturing the diamond nanoparticles. The Seoul Nat' team used a silicon monoxide membrane of the TEM Cu grid with capture times of 3, 6, 9, 12 and 15 s at the capture temperature of 600 °C and the hot filament temperature of 2000 °C under 20 torr. The STEM mode was used in Fig. 2, which could achieve a much higher contrast than the HRTEM mode. The white spots in Fig. 2 mean the captured nanoparticles. Because of the incoherently scattered electrons, the crystalline particles tend to appear bright.

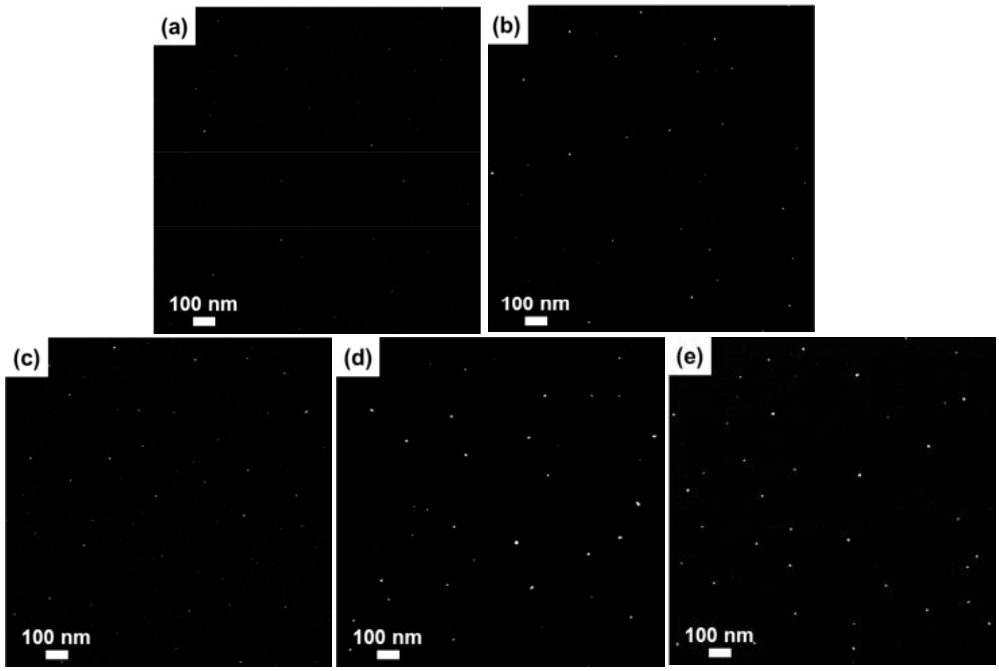

Fig. 2 STEM images of nanoparticles captured on the silicon monoxide membrane of the TEM Cu grid with

capture times of (a) 3, (b) 6, (c) 9, (d) 12 and (e) 15 s.

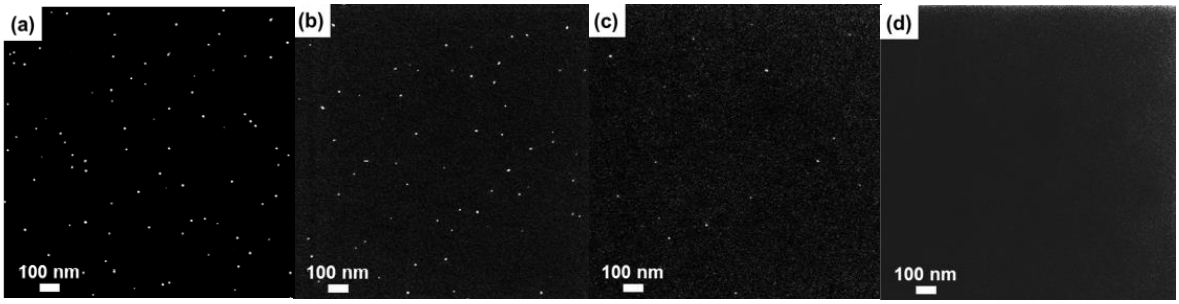

Fig. 3 STEM images of nanoparticles captured for 10 s on the silicon monoxide membrane of the TEM Cu grid at electric biases of (a) +75, (b) 0, (c) -75 and (d) -200 V.

Supposing that nanoparticles are charged in the chamber, the Seoul Nat' team anticipated that captured nanoparticles could be affected by bias. The electric bias was applied to confirm whether the nanoparticles are negatively charged or not, and the bias was applied to the stainless plate, which was below the quartz holder loaded with the TEM grid. Figs. 3(a)-(d) show the STEM images of nanoparticles. The nanoparticles were captured for 10 s on the SiO (silicon monoxide) membrane at the substrate teperature of 600℃ under the electric biases of +75, 0, -75 and -200V, with other experimental conditions being the same as Fig. 2. It is certain that the size of captured nanoparticles didn't change with decreasing electric bias from +75V to -200V. However, the number of captured nanoparticles decreased with decreasing electric bias from +75 to -200 V. The Seoul Nat' team found that there was no nanoparticle at the electric bias of -200 V in Fig. 3(d). As shown in Fig. 4, The number densities of diamond nanoparticles were 86, 40, 9 and 0 per μm^2 respectively for +75, 0, -75 and -200 V. Hence, the Seoul Nat' team could infer the negatively charged nanoparticles from the results of the Figs. 3 and 4. HRTEM was used to identify whether the captured nanoparticles have a diamond structure or not. Fig. 5 show the HRTEM images of nanoparticles captured for 15 s on the carbon membrane under the electric bias of +75 V with other conditions being the same as Fig. 2.

The dark spots in Fig. 5(a) show the nanoparticles. The nanoparticles of 4-6 nm are distributed randomly on a carbon membrane. The HRTEM image in Fig. 5(b) shows that the nanoparticle has a diameter of ~ 3.91 nm and 0.206 nm of crystalline lattice spacing, which indicates the spacing of {111} planes of diamond. The selected area electron diffraction (SAED) pattern recorded from the nanoparticles is shown in Fig. 5(c). From the lattice image in Fig. 5(b) and the SAED pattern in Fig. 5(c), it could be said that the captured nanoparticle has a single crystalline diamond structure.

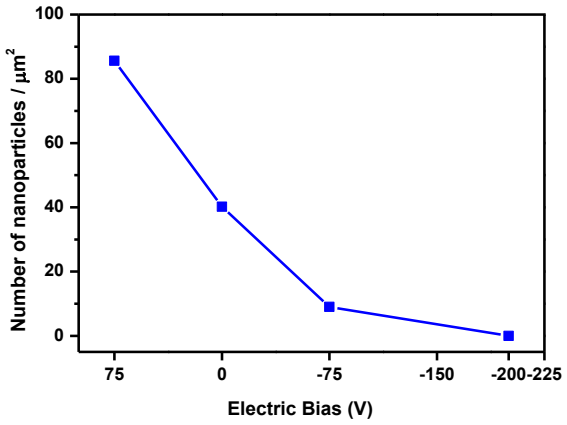

Fig. 4 Number density of nanoparticles captured for 10 s at electric biases of +75, 0, -75 and -200V.

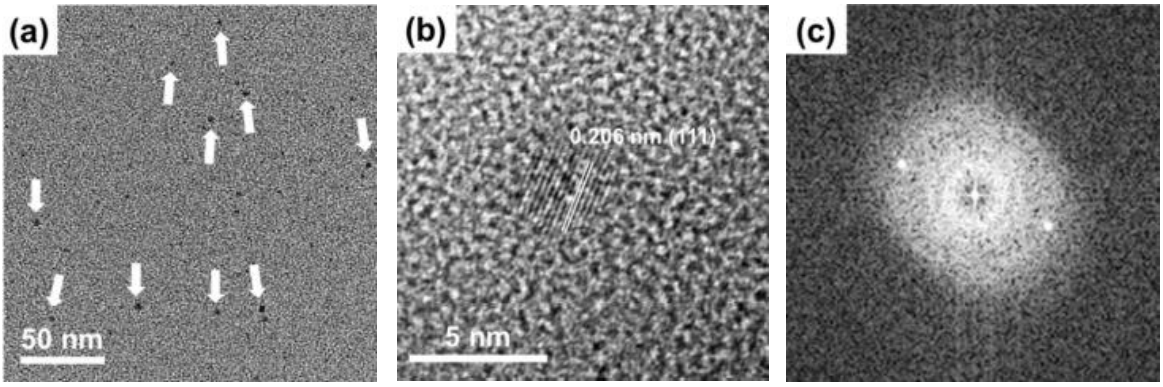

Fig. 5 (a) HRTEM image of nanoparticles captured for 15 s on the carbon membrane. Nanoparticles are indicated by the white arrows. (b) High magnification of (a) showing the crystalline lattice spacing of 0.206 nm, corresponding to the (111) plane of diamond. (c) The selected area electron diffraction pattern of the crystalline nanoparticle.

The results of Figs. 2, 3 and 5 show, that we can synthesize diamond nanoparticles of relatively uniform size HFCVD reactor under a particular condition of diamond deposition. This method of diamond nanoparticles can also be applied to the other low-pressure diamond deposition processes such as using plasma or flame. This result is related to the gas phase nucleation of diamond in the diamond CVD process reported by Frenklach et al. This report proves that diamond nanoparticles, which have been synthesized by the detonation process, can be synthesized also at low pressure under the typical processing condition of diamond films. This method has some advantages over the detonation process in that it produces non-agglomerated isolated diamond nanoparticles without additional processes such as de-agglomeration, milling and fractionation. Also, this process goes sequentially. Also, as to the purity of diamond nanoparticles, the lattice image in Fig. 5(b) and the SAED in Fig. 5(c) reveal that they have a single crystalline diamond structure without other carbon allotropes like graphite or amorphous carbon. Therefore, the captured diamond nanoparticles in Fig. 5(a) and (b) achieved high purity without any non-diamond phase. In addition, this method may bring other advantages regarding the control of size and the bigger scale of production. Considering the bias effect shown in Fig. 3, all of these diamond nanoparticles seem to be negatively charged.

Capturing charged diamond nanoparticles in the gas phase can provide a new approach to the synthesis of diamond nanowires. It would be a ground-breaking step to grow diamond nanowires in HFCVD. Moreover, it can be very significant results from another direction. This can be used to open the way that diamond nanoparticles doped silicon atoms will be reproducibly applied in single photon emission.

2) Trial growth for diamond nanowire by using HOPG

In order to find an experimental condition for the synthesis of diamond nanowires, understanding on the effect of many parameters was required such as gas-flow ratios, partial pressure, growth temperature, growth time, gas composition, and preparation of catalysts (materials, preparation methods, and initial sizes or thicknesses), and cooling rate and cooling gas flow rates. The Seoul Nat' team tried to find the stable equilibrium that can maintain the state of diamond nanowires. For example, the alloying approach can reduce an inter-diffusion coefficient and limit both bulk- and surface-diffusion. The cooling rate approach can determine a Gibbs free energy between graphite and diamond.

The Seoul Nat' team took the first step to find the catalyst metal that could solute a methane gas in catalyst, the Seoul Nat' team have been doing experiment using Fe, Ni, Pt coated diamond-silicon film that a diamond film was deposited on the silicon substrate. During the past year, the Seoul Nat' team has used APCVD and HWCVD for the synthesis of diamond nanowires using catalyst metals.

Many attempts were tried, and we could get some results. In this process we were able to obtain a peculiar form of SiC wires.

Under conditions where diamond was deposited, when doing for the growth of carbon nanotubes, accidentally we found a lot of form of wire bundle. At this time, the Seoul Nat' team knew that given these changes were affected by the small size quartz substrate, after that we tried to do experiments for analyzing the bundle. There were insensible changes about a bundle, even though methane concentration was changed. The Seoul Nat' team did an experiment with HOPG which was a source for carbon and got an amazing result from bundle.

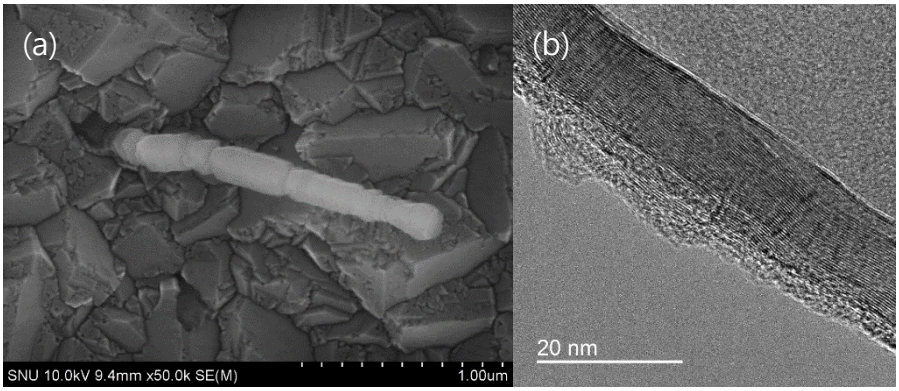

Fig. 6. (a) SEM image of SiC nanowire, (b) TEM image of SiC nanowire grown by using HOPG. The nanowire was grown at at 970 ^{o}C for 2 h with a gas flow ratio of H_2 100 - CH_4 0 sccm

The Seoul Nat' team could get 1-dimension wires from the result, which is suspected as diamond nanowires at first time. Climbed higher, the structure turned out to be a thinner form. It meant that particles were grown from a catalyst metal. The Seoul Nat' team anticipated that an image force was essential in the growth of diamond nanowires in HFCVD. Therefore, we conjugated that this type of wire would be an ideal form of diamond nanowires if diamond nanowire was synthesized in HFCVD by TCN. However, the Seoul Nat' team couldn't could not be convinced that the nanowires had a diamond structure because it was not known whether an atom consisting of the wires came from HOPG or from charged nanoparticles in the gas-phase. To analyze the wires more precisely, the Seoul Nat' team tried to do additional experiment under other experimental conditions. It was really hard to get a TEM sample because the wire was very brittle and sensitive. So the TEM grid could be sampled by FIB (Focused Ion Beam – Quanta 3D). Through the TEM analysis, we came to know that the wires were made up of graphitic surface and the core of the SiC crystal structure. The synthesis of SiC wires was already reported in HFCVD, but the image of Fig.6(a) showed that the wire structure was different from known SiC wires whose shape was sharp and linear. It looked like that the wire in Fig.6(a) had grown by nanoparticles, resulting in 1-dimension wire formation. In addition, the TEM image of Fig. 6(b) showed the lattice image of the wire structure unlike carbon nanotubes; the SiC nanowire possesses a solid wire instead of a hollow tube structure.

3) Artifacts problem on TEM grid

After the Jin-Woo Park's success to capture the diamond nanoparticles in the gas phase, Hwan-Young Kim and Byung-Kwan Song who were follow up members of Jin-Woo Park's study had tried to capture the diamond nanoparticles reproducibly. When Hwang's group succeeded to capture nanodiamonds, unusual phenomena took place on TEM grid (carbon membrane, TED PELLA, INC.)

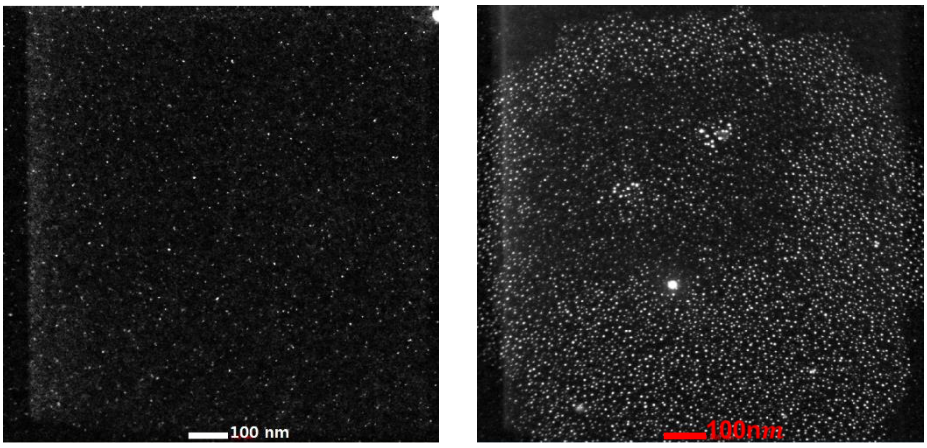

Fig. 7 STEM images of nanoparticles captured on the carbon membrane of the TEM Cu grid. Left(a) was captured by Dr. Jin-Woo Park, Right(b) was captured by Hwan-Young Kim and Byung-Kwan Song.

The Seoul Nat' team had tried to analyze the phenomena for proving whether the phenomena were related to electron-particles interaction or contamination problem. But those group shapes were not always captured on TEM grid. The Seoul Nat' team analyzed bare carbon membrane of the TEM Cu grid to clarify the problem and tried to find contamination on membrane and check whether chamber was contaminated or not. But, there was clean membrane and there wasn't contamination in chamber. It was hard work to understand the group phenomena. After we had a confidence that there was no contamination of chamber and no evaporation possibility of mesh which was consisted of Cu (melting point was at 1358K). We tried to analyze the bare TEM grid again. And we knew that both clean membrane and contaminated membrane were existed on bare membrane. Comparing with the results of Figs. 8 and Fig. 9(b) shows the possibility that charged nanodiamonds were preferentially deposited on the artifacts.

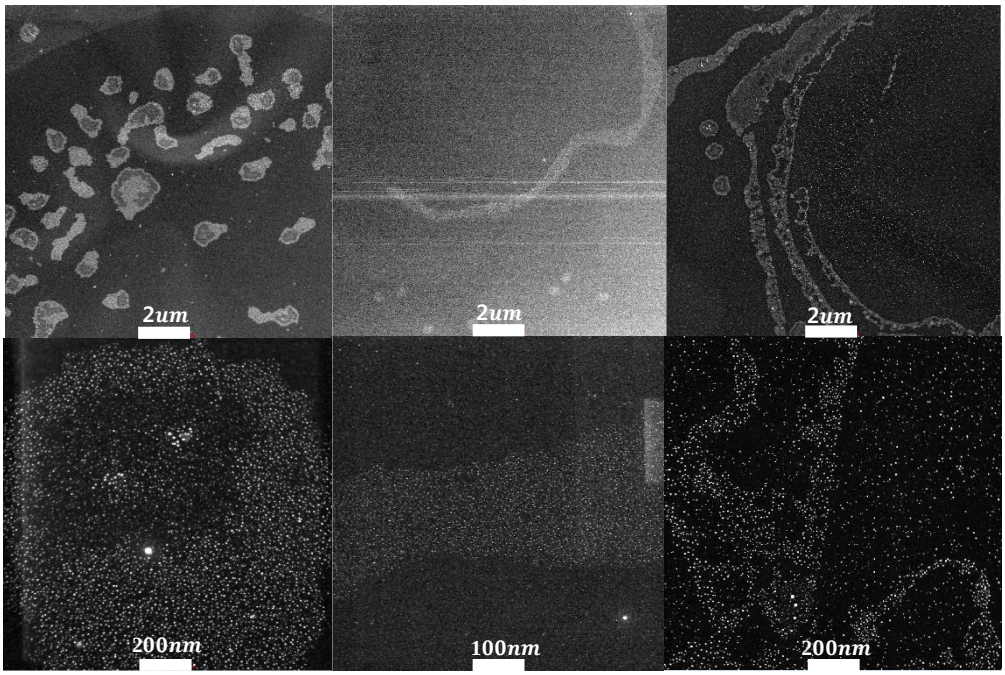

Fig.8 STEM image of nanoparticles captured on the carbon membrane of the TEM Cu grid. There were various shapes of group nanoparticles on TEM grid.

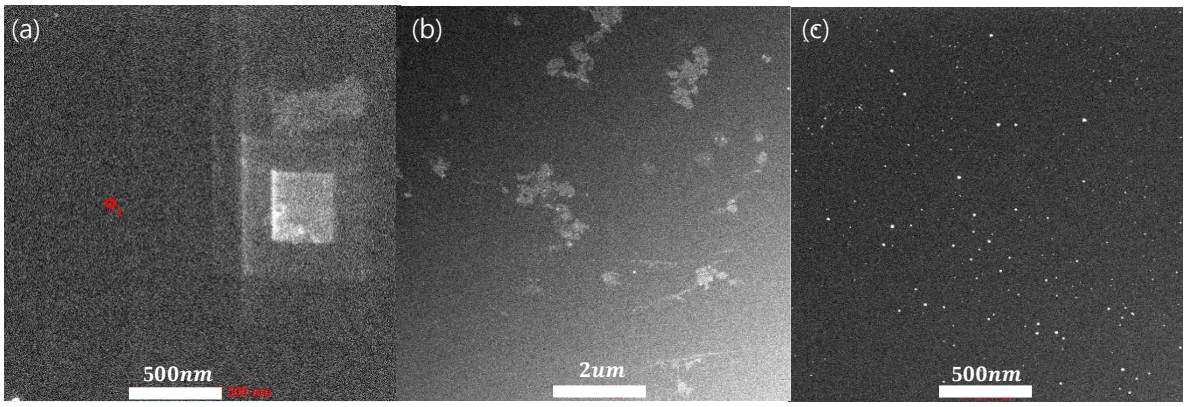

Fig. 9 STEM images of bare membrane on TEM Cu grid. (a) was a clean sample, (b) had gray artifacts, and (c) had a lot of bright artifacts particles.

4) Unusual d-spacing problem of nanodiamond

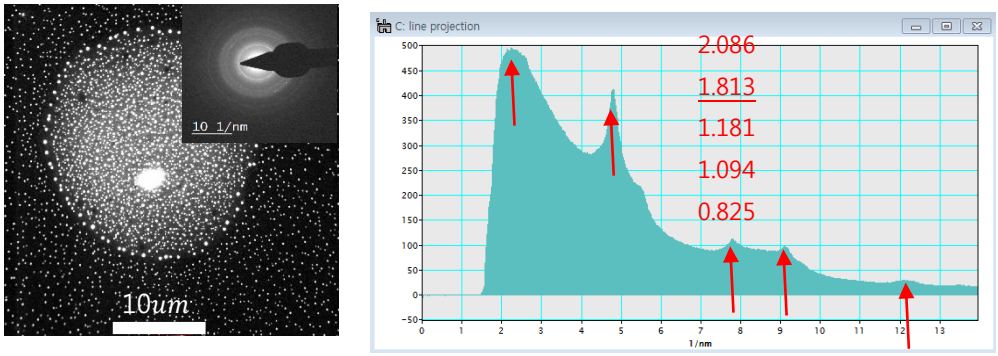

Fig. 10 Group nanoparticles with ring pattern of diffraction analysis(left) and Intensity of d-spacings of ring parttern(right).

The 1.813 angstrom in Fig. 10 (right) was abnormal d-spacing in perfect diamond. 1.813Å were related with {200} plane and usually shown in n-diamond or lonsdaleite structure. Hwang's group suspected various possibilities. It would be occurred by contamination from Cu mesh which had low melting point. So several kinds of mesh, Mo, Ti and Pt which had higher melting point than Hot-filament temperature-almost 2400k, were used to determine whether the particles were contaminated or not. We found that 2.2Å and 1.813Å d-spacing were observed in all mesh. And Hwang's group deposited particles at capture condition, at 2500K filament temperature, 875K capture temperature, 20 torr pressure and not 15 seconds, but 4 hours. And the deposited particles showed carbon peak in Raman analysis(LabRAM HV Evolution). Although, Fe, Ni and Cu mesh also had similar d-spacing with lonsdaleite or cubic diamond, however, raman peak of deposited particles were only on carbon peak. And if they were evaporated, they should appear on all TEM grid. But, the artifacts didn't appear on the all samples. Therefore, possibility that the particles were came from mesh or electrode metal was unlikely. The HRTEM images in Fig. 8 show that the nanoparticle has ~ 3.9 nm of diameter and 0.227~0.185 nm of crystalline lattice spacing, which indicates {111} and {200} planes of diamond. From the lattice images and d-spacing informations in Fig. 8, it can be said that the captured nanoparticle has a possibility that it's crystal structure would be similar with lonsdaleite or cubic diamond.

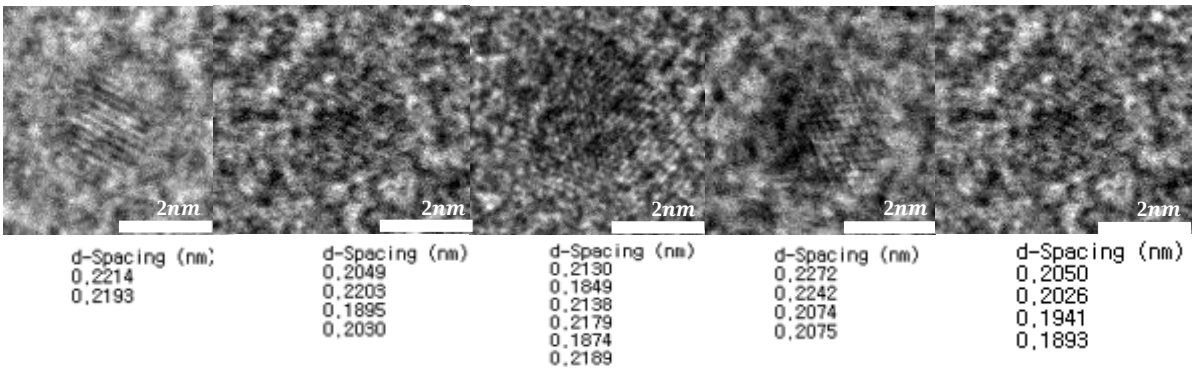

Fig. 11 D-Spacing information and crystal structure of nanoparticles captured for 15 s at 600 ºC capture temperature

5) Liquid like property of charged nanoparticles

Growth mechanism of charged particles could be an approach to understand quality of micro-diamond. On the base 'charged cluster model', most probability of the quality would be close to crystal structure of building block itself. Fig. 9(a) and (b) is one of puzzling phenomenon in the diamond CVD process. Diamond films or crystals grow on a silicon substrate while highly porous and skeletal graphitic soot particles grown on an iron substrate under the same deposition conditions as shown in figure Fig. 12. Skeletal and crystal diamond suggest that charged nanoparticles were affected by charging rate on substrate – Insulating substrate(Si) can maintain high electron density on substrate rather than conducting substrate(Fe). Hwang's group called it 'liquid like property.'. And Hwang's group formulated a hypothesis that formation of charged cluster was transformed when the charged particles reached substrate.

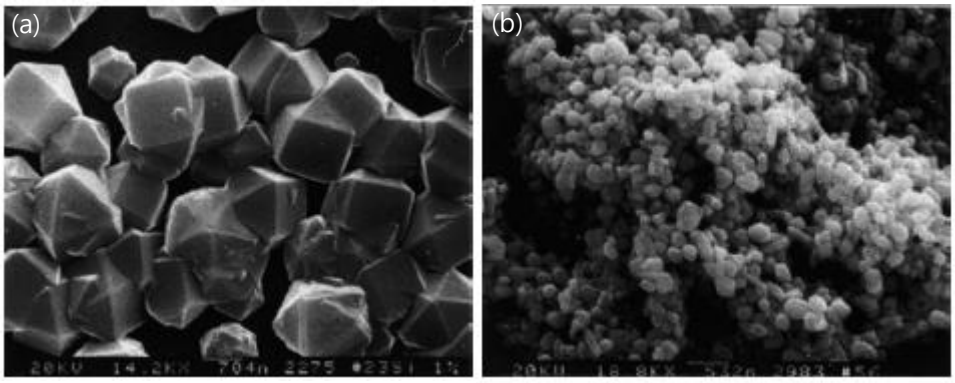

Fig. 12 (a) Diamond deposited on a silicon substrate and (b) soot deposited on an iron substrate with 1%CH_4-99%H_2 gas misture for 2h at a substrate temperature of 990℃ under 2700Pa (SEM): substrates were placed side by side during hot wire diamond CVD. Copyright 1996 Elsevier.

In fig 12(a), when charged nanoparitcles reached on substrate, the particles can hold charge long time. And this property gave particles time and energy for transformation between charged particles to diamond nanoparticles. On the other hand, fig 12(b) meant that the charged particles would lose charge rapidly compared with the particles on insulating substrate.

For clarify the liquid like property associated with crystallinity of nanoparticles captured on

substrate, experiments were designed to control the relation between charged nanoparticles and electrons trapped on substrate. Fig 13 (a) and (b) showed that liquid like property of charged nanoparticles affect the crystal structure of charged nanoparticles. Size of the particles on the graphite flake on Fe were usually bigger than the particles on the graphite flake on Si. And d-spacing were not well observed.

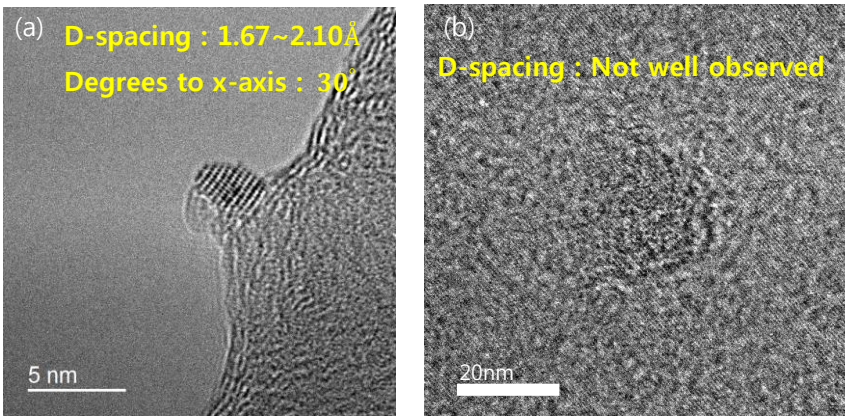

Fig. 13 HRTEM image of nanoparticles captured for 15s on the graphite flake at 720℃. Fig (a) was captured on the graphite flake on insulating substrate (Quartz) showing the crystalline lattice spacing of 0.167~0.210 nm, fig (b) was captured on the graphite flake on conducting substrate(Fe)

For capturing the nanodiamond generated in gas phase above 900℃, Hwang's group found an idea. Since SiO membrane of the TEM grid was so weak at temperature above 650 ℃ and the capture temperature was etching condition to carbon membrane of the TEM grid, so we used small piece of flake of graphite attached to carbon membrane of TEM Mo grid. Even though carbon membrane was etched at 900℃, small piece of flake wasn't etched not all of them. Hwang's group could analyze the captured particles on small piece of graphite flake. Experiments were worked at 900℃, 820℃ and 720℃ capture temperature, 1% methane concentration, and other experiment conditions were same to Jin-Woo Park's capture condition. As you can see that their shape and crystallinity were different each other. D-spacing of the particles in fig 14(b) had a 2.76~3.47Å and d-spacing of the particles in fig 14(c) had a 1.67~2.10 Å. The purpose of capture at 900℃ was to capture a high quality diamond nanoparticles. Because temperature above 900℃ was a condition to synthesis high quality diamond film or particles. However, it was hard to analyze the particles. Those particles were gathered together with large black debris. But those debris were decreasingly appeared in sample fig 14(b), (c). Because driving force for etching of carbon atom at lower temperature was higher than at high temperature. So carbon debris would be etched atomically by decreasing capture temperature.

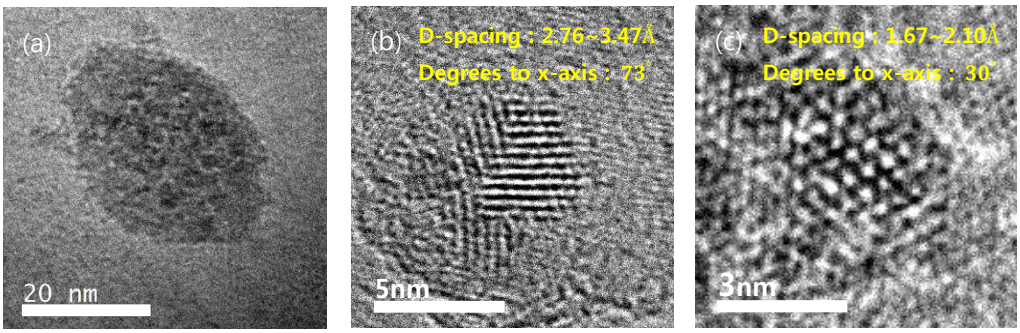

Fig. 14 HRTEM image of nanoparticles captured for 15s on the graphite flake on Quartz at 900℃(a), 820℃(b), 720℃(c). D-spacing of the particles in sample (b) was 2.76~3.47Å and degrees to x-axis was 73°. D-

spacing of the particles in sample (c) was 1.67~2.10 Å and degrees to x-axis was 30°.

6) Trials for SiV nanodiamnd.

Hwang's group thought that liquid like property of charged nanoparticles was main problem in order to synthesize the SiV nanodiamond. To solve the problem, Our group had tried to do many trials, such as capture diamond nanoparticles on TEM grid and Si substrate during 5~15sec, deposit diamond nanoparticles on Si substrate during 1~10 min, capture diamond nanoparitcles on flake of graphite on Si substrate. Each method has an advantage and problems. Contaminaiton and resolution of SEM were a problem when diamond nanoparticles were captured on Si substrate. Because those were so small(~5nm) that it was difficult to analysis by using SEM. So Hwang's group tried to analysize the sample by using ATM, but it was difficult to compare nanodiamond with small artifacts on Si substrate.

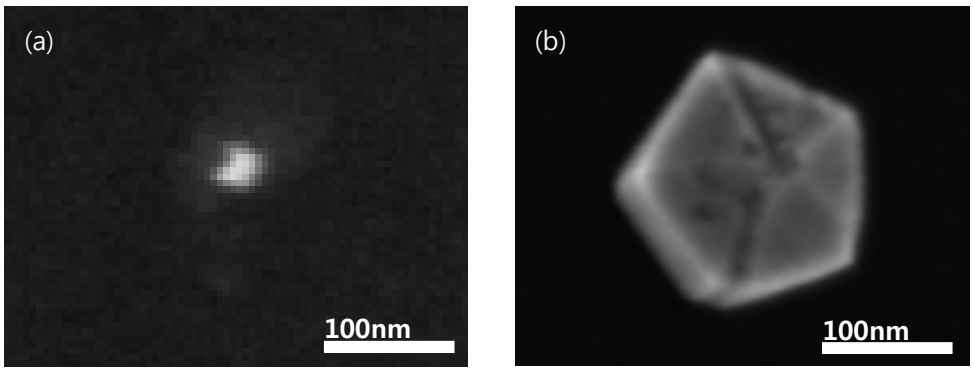

Fig. 15 SEM image of nanoparticles deposited on Si substrate for 10min(a) and 30min(b) at 950℃ substrate temperture and 1% methane concetration with diluted silane 0.06sccm. (Ratio of silane/methane was 60ppm)

Hwang's group had tried for synthesis of nanodiamond by controlling deposition time. In fig15(a), (b), diamond was deposited for 10min and 30min. When deposition time was short such as 1min, diamond nanoparticles were not well observed. But Hwang's group thought that decreasing deposition time was right direction for nanodiamond(~5nm). Simultaneously, even though liquid like property was problem, capture method wiil be tried again for preparation to the SiV nanodiamond.

As the size of nanodiamond get smaller, understanding the formation mechanism of these diamond nanoparticles is critically important to synthesize SiV nanodiamond. However, the relation between liquid like property and crystallinity of nanodiamond has not been understood yet. There were many problems to success to find the liquid like problem in SiV nanodiamond. It looks like final problem to make doping nanodiamond, but new problems will be appeared as it has always been. Capturing charged diamond nanoparticles in the gas phase can be a possibility to provide a new approach to the synthesis of SiV diamond nanoparticle.

7) Efforts to synthesize cubic nanodiamonds on graphite flake and SiO_2 membranes

In Year-1, the SNU team succeeded in capturing nanodiamond particles and confirmed that the nanoparticles were negatively charged.At that time, however, the team believed implicitly that captured nanodiamonds have a cubic diamond structure, not paying much attention to the possibility of many allotropes of diamond nanoparticles. In Year-2, the team made efforts to identify the crystal structure for d-spacings such as 1.8 Å, 2.2 Å and 2.4 Å, which do not belong to those of cubic diamond. In Year-

3, the effect of methane concentration on the size and structure of nanodiamonds was studied. It was found that at low methane concentration (1%CH_4), nanodiamonds have d-spacing close to that of cubic diamond and at high concentration (3%CH_4), nanodiamonds have d-spacing close to that of hexagonal diamond or graphite.

Basically, the time for capturing nanodiamonds was 15 sec. For an insulating SiO_2 membrane, which was damaged less than SiO and carbon membranes, nanoparticles could be hardly found for the capturing time of 15 sec at 900^{o}C and 1%CH_4. In this case, capturing time was extended to 60 sec and then some nanoparticles could be observed on the SiO_2 membrane. Nanoparticles have a size range of 3 ~ 6 nm with d-spacing of 1.75, 1.86, 2.06, 2.2 and 2.4 Å.

Similar nanoparticles were observed on a graphite flake membrane for the capturing time of 15 sec at 900^{o}C and 1%CH_4. In addition to these nanoparticles, some abnormally large nanoparticles of 7 ~ 12 nm were also observed, which have an amorphous structure revealed by the TEM analysis. When the capture was extended to 60 sec, however, these abnormally large nanoparticles were not observed, indicating that they were etched away. Abnormal nanoparticles which were captured at 1% methane concentration were not captured on the graphite flake at 3% methane concentration. The results about the nanoparticles at 3% methane will be discussed. Moreover, the team tried to understand the relationship between high temperature condition and crystallinity of diamond nanoparticles.

In parallel, the Seoul Nat's team has tried a new approach to understand the crystal structure of nanoparticles. In charged nanoparticle theory, it was expected that charged condition of nanoparticles would determine size and stability of diamond nanoparticles, which related with the etching rate of diamond particle. The surface of tungsten wire can significantly change the electron density in the system. And the wire surface had a different work function due to graphitic carbon complex on the wire. Surface ionization related with the amount of C_2 negative radical in the system. Saha-Langmuir equation was used to get the work function of tungsten surface. If the growth rate of the diamond particles was inversely increased, the nanoparticles which had large size and unstable crystal structure would be etched easily. From the result which showed that charged condition was one of the main parameter to get the cubic diamond nanoparticle, the Seoul Nat's team has been getting closer to the cubic nanodiamond.

The experimental condition was same with the condition which high quality diamond deposition was usually occurred. (Filament temperature 2100 ^{o}C, temperature at capture 900 ^{o}C, 20 torr and 1% methane concentration.) Fig.16 (a) and (b) showed the results which were captured at the condition. There were several kinds of nanoparticles on graphite flake mesh.

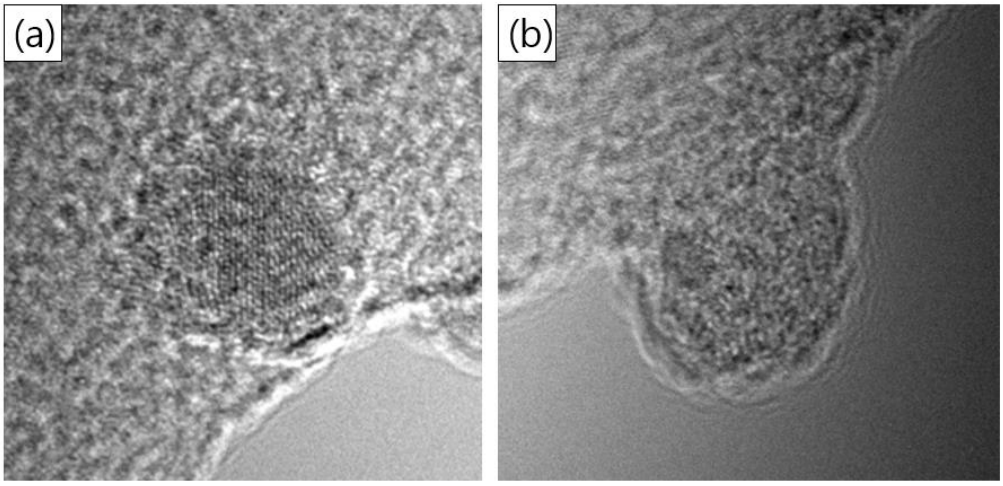

Fig. 16. TEM images. (a) and (b) nanoparticles were captured on the same mesh sample during 15sec. (a) nanoparticle had a crystal information, but (b) nanoparticle was amorphous structure and bigger than (a) nanoparticle.

The kind of nanoparticles (a) had a crystallinity and usually showed 2.40Å, 2.16Å, 2.06Å, 1.98Å and 1.75Å which were related with the diamond like carbon structure. Most values were 2.06 and 1.98, but 1.75Å was related with hexagonal diamond structure. Size of the nanoparticles(a) was 3~6nm,

however size of the nanoparticles(b) was 7~12nm. Some nanoparticles which had a big size(10~20nm) and crystal structure existed, but ignore those in the report. Because those nanoparticles were outside of the gas phase generation of nanoparticles.

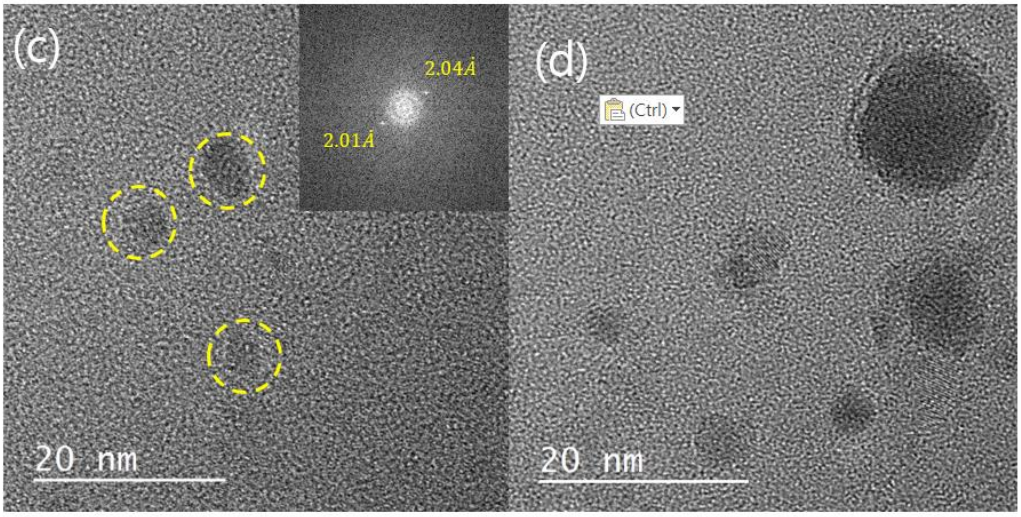

Fig. 17. (c) and (d) capture time was 60 sec. The size of the nanoparticles was almost 3~6nm. Some nanoparticles were grown(d) The TEM grid was PELCO ®. Silicon Dioxide Support Films for TEM. Ted Pella Inc.

To confirm the nanoparticles, 60 sec capture time was used. If the nanoparticles were not growth unit of the particle, the small size of the nanoparticle would not exist when the capture time was long. Even the time was long, the small particles were also observed. And silicon dioxide mesh was used to hold from a thermal damage for long capture time. The nanoparticles (b) were not observed when the capture time was long. The Seoul Nat's team suspected that the amorphous structure of the nanoparticles was easily etched by atomic etching process. In the theory of charged nanoparticles, unstable sp2 bonding related with graphite like structure and had a driving force for phase transition from solid to gas. The nanoparticles (c) showed 2.31Å, 2.21Å, 2.01Å and 1.98Å. The 1.75Å d-spacing was related with a forbidden plane in hexagonal diamond, but not observed. Some nanoparticles size (d) had almost 20nm which were grown during capture time 60 sec.

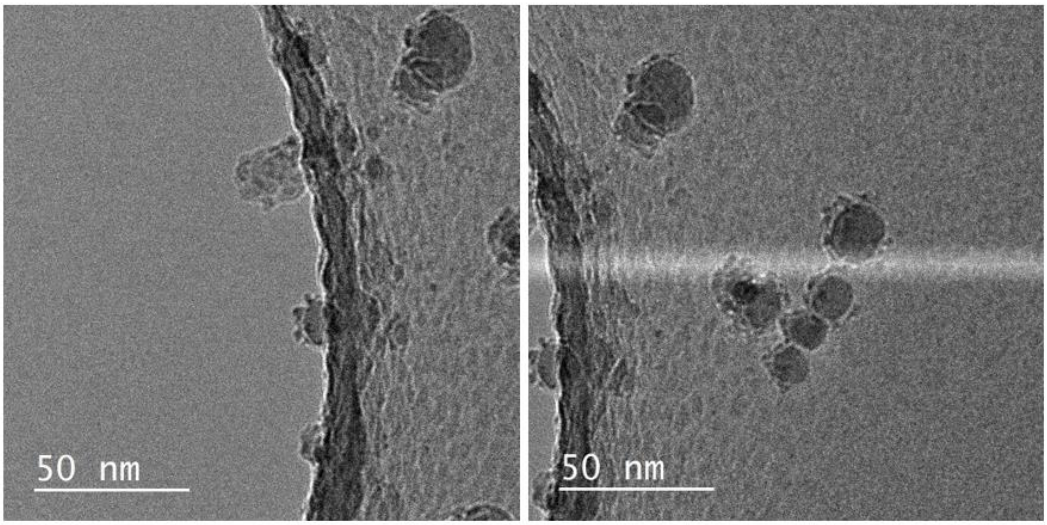

Fig. 18. Nanoparticles captured for 15sec and at 900 ºC and delay time 15min. Graphite flake membrane was used to help in endure high temperature.

The purpose of delay time was to confirm the gas phase generation of nanodiamonds. The holder for capturing nanoparticles was exposed for 15min with holder cover on it which prevents the nanoparticles from capturing on the membrane. After delay time, the holder cover was moved away

and the nanoparticles were captured on the membrane. The result of delay time method was shown in fig. 18. The size of the nanoparticles was from 10nm to 20nm. And the small nanoparticles(2~3nm) were attached on the surface of the large nanoparticle(10~20nm). The morphology of the nanoparticles shown at fig. 18. was rough and cauliflower structure. The discrepancy of the tendency of nanoparticles between the nanoparticles for no delay time and for 15min delay time implicitly told us that the nanoparticles were agglutinated at the gas phase.

The Seoul team also compared with the growth particles and captured nanoparticles. When the diamond particle was grown, the particle had d-spacing of cubic diamond. But the nanoparticles (a)~(d) had unusual d-spacing of cubic diamond. Christoph G. Salzmann and Benjamin J. Murray studied the hexagonal diamond 3 years ago. And they focused on the fraction of hexagonal stacking in the hexagonal diamond. Peter Nemeth, Laurence A.J. Garvie and Peter R. Buseck studied the defects in cubic diamond. And they explained that the values of d-spacing of lonsdaleite were related with the defects in cubic diamond. The Seoul team also considered that the unsual d-spacing would be related with the lonsdaleite and defects in the diamond like nanoparticles.

The nanoparticles which were captured at 1% methane concentration and low temperature had 1.67~2.06Å d-spacing which meant that crystal structure of the nanoparticles was close to cubic diamond. Even though nanoparticles had bcc structure, but they had forbidden value 1.67Å. Size of the nanoparticles at high temperature was bigger than at low capture temperature, and close to lonsdaleite diamond structure. And decreasing size of the nanoparticles was a good match for thermodynamic calculation. But some problems were happened at 3% methane concentration.

8) Unexpected phenomena of nanoparticles at 3% methane concentration.

The nanoparticles at high temperature were close to graphite like carbon structure. And they had a tendency that average d-spacing of nanoparticle was increased which means that they have a different crystal structure. Unlike at 1%, the nanoparticles at 3% were grown by decreasing of capturing temperature. Size of the nanoparticle at 1% was changed from 3~6nm at 900 °C to ~3nm at 600 °C, but the size at 3% was changed from ~3nm at 900 °C to ~5nm at 600 °C. The table 1 summarized the crystal information of the nanoparticles, which were captured under 3% methane concentration.

The SNU group thought the non-diamond nanoparticles were etching while far away from the filament. And the thermodynamic simulation by Thermo-Calc version Q also supported that the etching driving force at 600 °C was much higher than at 900°C. From this point of view, it is possible to explain the decreasing size of the nanoparticles at 1%. However, size of the nanoparticles at 3% was increased as decreasing filament temperature. Results showed that average size of the nanoparticles was ~3nm at 900 °C and 3~5nm at 600°C. This meant that the nanoparticles were grown at the gas phase. Addition to this, the values of d-spacing were also changed. The values at 1000 °C showed 2.61Å, 2.53Å, 2.48Å and 2.23Å. But crystallinity was changed from those to 2.27Å, 2.17Å, 2.06Å, 1.88Å and 1.78Å. To understand the tendency, phase transformation of nanoparticles should be assumed.

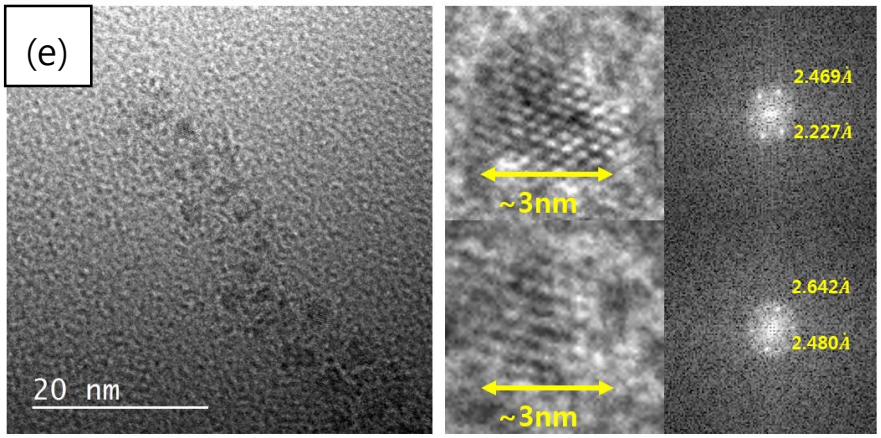

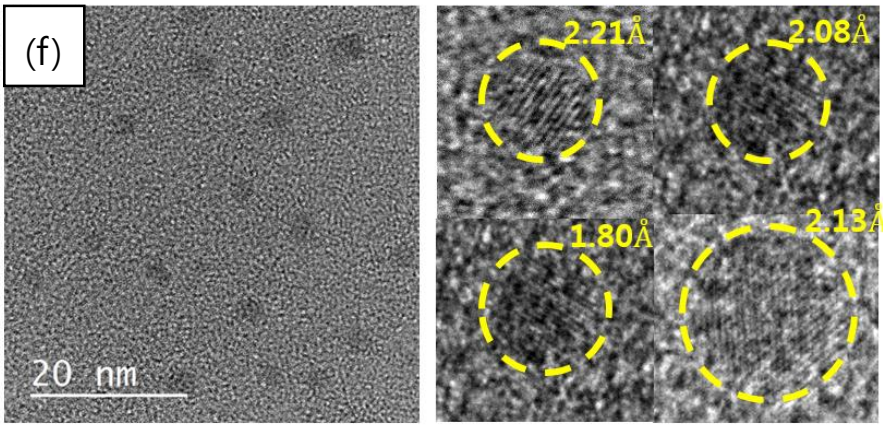

Fig.19. (e) was the nanoparticles captured at 1000 ºC and (f) was the nanoparticles captured at 600 ºC. Average size of the nanoparticles was ~3nm at 1000 ºC and ~5nm at 600 ºC. The nanoparticles at 1000 ºC also showed allotropes of diamond structure.

1000°C (Experimental)	900°C (Experimental)	600°C (Experimental)	400°C (Experimental)	Cubic diamond (JCPDS 6-0675)	Hexagonal diamond (19-0268)	Graphite (00-056-0159)
						3.35 (002)
2.619						
2.48~2.53	2.488~2.57		2.55			
2.228	2.145	2.17~2.27	2.10~2.24		2.18 (100)	2.13 (100)
		2.06~2.11	2.03~2.06	2.06 (111)	2.06 (002)	2.03 (101)
		1.88~1.94			1.93 (101)	
		1.78~1.83		1.78 (200†)		1.67 (004)
					1.50	
				1.26 (220)	1.26	1.26
					1.17	

Table 1. the values of d-spacing of captured nanoparticles. The nanoparticles were captured at different capture temperature and compared with diamond structure.

The stability of nanodiamond in response to external stimuli was already studied a lot. And the kinds of stimuli were related with annealing, thermal activation, pressure, irradiation-induced transformations, time, and charge. Heat-induced transformation of nanodiamond was studied by MD simulation, phase transformation of diamond was also related with temperature dependence. Moreover, the size stability of diamond was depended on the thermal energy. The bigger nanodiamond is, the more stable it is at high temperature. M.Y. Gamarnik studied the size-temperature dependence of nanodiamond. He showed that almost 10nm diameter of nanodiamond was stable at 1000 ºC, so the captured nanoparticles at 900 ºC 1% which had a size distribution from 3 to 6nm would be explained by this point of view. But the nanoparticles at 3% were not explained by using the thermodynamic calculation and MD simulation. SNU group had not a confidence what was the true. But some practices were done.

9) Unusual dependence of diamond growth rate on methane concentration in HFCVD.

If the amount of precursor was increased, the growth rate would be increased. This natural intuition was also happened on the diamond growth rate. When the methane concentration was

increased from 1% to 3%, the size of the grown particle was also increased. But those things were only happened at filament temperature 2100 ºC. When the filament temperature was decreased below 2000 ºC, the diamond growth rate was decreased even though the methane concentration was increased from 1% to 3%. What would happen?

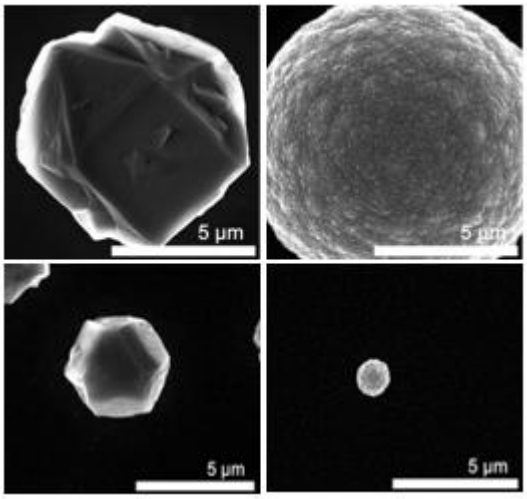

Fig.20. Above images showed the particle grown at filament T 2100 ºC. Left (1%), right (3%). Below images at filament T 1900 ºC. Left (1%), right (3%).

To investigate this behavior, nanoparticles existing in the gas phase were directly captured with TEM grid, in order to see if there is any change when the filament temperature is lowered, since thery become building blocks for diamond film. Furthermore, surface condition of the filament and its emission of electricity was investigated to understand environmental factors of the formation of charged nanoparticles. As methane concentration increases and filament temperature decreases, the filament gets poor in charging clusters nearby, and therefore the growth rate of diamond plummets.

As methane molecules pass through the hot filament, it decomposes into carbon atoms and various carbon-hydrogen compounds, and some of them gathers to nucleate into carbon clusters. These carbon clusters are stabilized in diamond phase, thanks to electrons emitted from the hot filament. As mentioned above, excess charge in carbon clusters makes diamond phase more preferable.

In order to investigate why the dependence of diamond growth rate on methane concentration was inversed as filament temperature was lowered below 2000 ºC, various approach had been made. Based on the theory of charged nanoparticles, we hypothesized that huge difference in nanodiamonds existing in the gas phase would be observed. Existence of nanodiamonds and their property of being negatively charged have been reported by Jin-Woo Park. We assumed that drastic decrease of diamond growth rate upon decreasing filament temperature in 3% methane concentration may have been resulted from huge difference or degradation of nanodiamonds in the gas phase. Therefore, experiments on directly capturing these nanodiamonds have been conducted for each processing conditions, for filament temperatures below 2000 ºC and above 2100 ºC, and for methane concentration of 1% and 3%. Ambient temperature at capturing zone was around 550 ºC. After capturing nanoparticles with TEM gird, it has been analyzed with TEM (Tecnai F20 and JEM-2100F).

It is important to know how much carbon clusters near the hot filament are negatively charged, since the excess charge in the carbon clusters affects weather they remain as diamond or transform into graphite. For this, thermionic emission current from the filament was measured. Thermionic emission current was measured at the same position as the capturing experiments, since too high temperature can cause phase transformation of the iron probe or generation of large thermoelectricity inside the probe. Also, tungsten wire can change its phase by absorbing carbon and thus change its electric resistance during the measurement if ambient temperature is too high. In addition, surface morphology of the filament used for the experiments was observed with optical microscope. On the surface of the filaments used in high methane concentration, precipitates could be observed with naked eyes.

Significant difference was observed between nanoparticles captured when the filament temperature was 1900 °C, as expected. Firstly, nanoparticles captured when the filament temperature was 2000 °C were single crystalline nanoparticles with size 3-5nm. Measuring lattice parameters of each particle, we found that these particles had d-spacing values of 2.1Å, 2.2Å or 2.5Å. Since (111) plane of diamond structure has 2.07Å, 2.1Å can be estimated to (111) plane of diamond. 2.2Å may indicate (100) plane of lonsdaleite, also called as hexagonal diamond. Lonsdaleite is an allotrope of carbon, which has diamond structure as main matrix but occasional structural defect of hexagonal sequences. Lastly, 2.5Å value has not been clearly determined. However, considering that only carbon atoms and carbon molecules exist in the gas phase, we assumed that these nanoparticles are another allotrope of carbon, named 'non-diamond carbon' particles. The percentage of appearance of each d-spacing values were 18%, 41%, 41% for 2.1Å, 2.2Å and 2.5Å, respectively.

On the other hand, nanoparticles captured when the filament temperature was 1900Å show completely different morphology as shown in Fig. 20-24. It has been observed that these nanoparticles were polycrystalline, with size up to 12nm, which is far bigger than nanoparticles captured when the filament temperature was 2000 °C. Since these nanoparticles become building blocks for diamond film deposition, we believe that this difference has contributed to severe decrease in growth rate of diamond in 3% methane concentration, when the filament temperature was lowered from 2000 °C to 1900 °C. Mueasurement of lattice parameters of these polycrystalline nanoparticles has shown that they also contain values of 2.1Å, 2.2Å and 2.5Å, but all of them existing simultaneously in one cluster. Moreover, their percentages of appearance were 6%, 19%, 75% for, 2.1Å, 2.2Å and 2.5Å, respectively. Notice that the fraction of 2.1Å, which indicates diamond nanoparticles, has severely decreased.

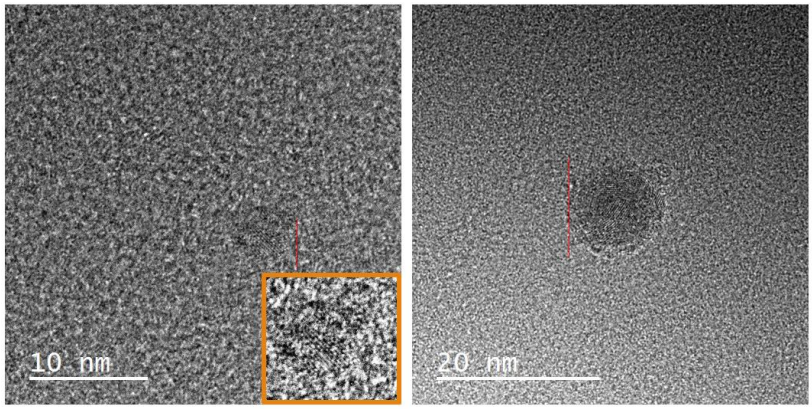

Fig. 21. Carbon nanoparticle captured when the filament temperature is 2000 °C(Left) and 1900 °C(Right). Size of the nanoparticle is around 4nm and 12nm.

Fig. 22. Shows the result of measuring thermionic emission current at each filament temperature in each methane concentration. The result clearly shows that thermionic emission increases with increasing filament temperature and decreases with increasing methane concentration. When temperature of the filament was 1900 °C, the measured currents were -0.49 uA/cm^2 for 3% methane concentration, and -7.10 uA/cm^2 for 1% methane concetration. In this case, thermionic emission increased by 1300% when methane concentration was reduced from 3% to 1%. When temperature of filament was 2000 °C, the measured currents were -2.55 uA/cm^2 for 3% methane concentration, and -9.39 uA/cm^2 for 1% methane concentration. This is an increase of 268%. Lastly, when filament temperature was 2100 °C, measured currents were -5.57 uA/cm^2 for 3% methane concentration, and -17.3 uA/cm^2 for 1% methane concentration. This is an increase of 210%.

Large difference in the amount of thermionic emission in 1% and 3% methane concentration appeared when the filament temperature is 1900 °C. Moreover, when methane concentration was maintained the same, current emission increased exponentially as the temperature of the filament increased, following the law of thermionic emission by Richardson.

Reason for the difference in current emission in different methane concentrations seems to be caused by difference in surface condition of the filaments. Direct comparison of surface morphology of the filaments used in methane concentration of 1% and 3% is shown in Fig. 23. When methane

concentration is 3%, carbon precipitates are observed on the surface of the filament, whereas the surface of the filament used in 1% methane concentration is clean. Fig. 23. Shows that these precipitates have been confirmed as carbon chunks, possibly graphite.

Thermodynamic calculation has been done to explain the difference in surface conditions of the filaments, shown in Fig. 20. It has been confirmed that in methane concentration of 3%, carbon in the gas phase precipitates to solid state at temperature below 2300 °C, whereas in 1% methane concentration, carbon precipitates on the filament at temperature below 2050 °C. Though carbon precipitates were not found on the filament used in 1% methane concentration and temperature below 2000 °C, the calculation partly explain why carbon precipitates exist only on the filament used in 3% methane concentration. It needs to be concerned that the calculation was conducted assuming perfect carbon-hydrogen system without impurities that might activity of carbon in the gas phase, and that the result is only a reflection of thermodynamic stability, which does not consider kinetic barriers.

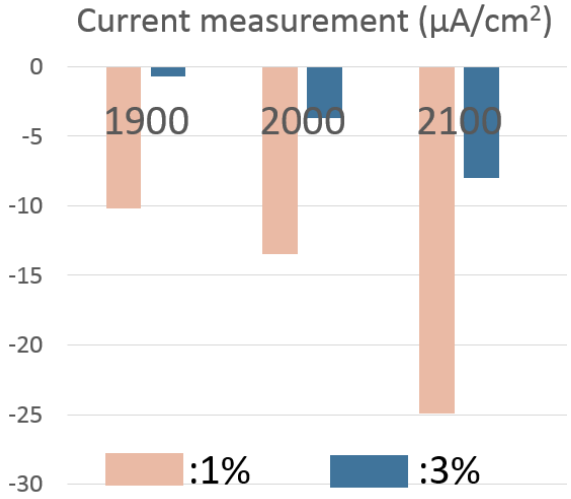

Fig. 22. Measurement of thermionic emission current in the filament temperature of 1900 °C, 2000 °C, and 2100 °C in methane concentration of 1% and 3%, respectively.

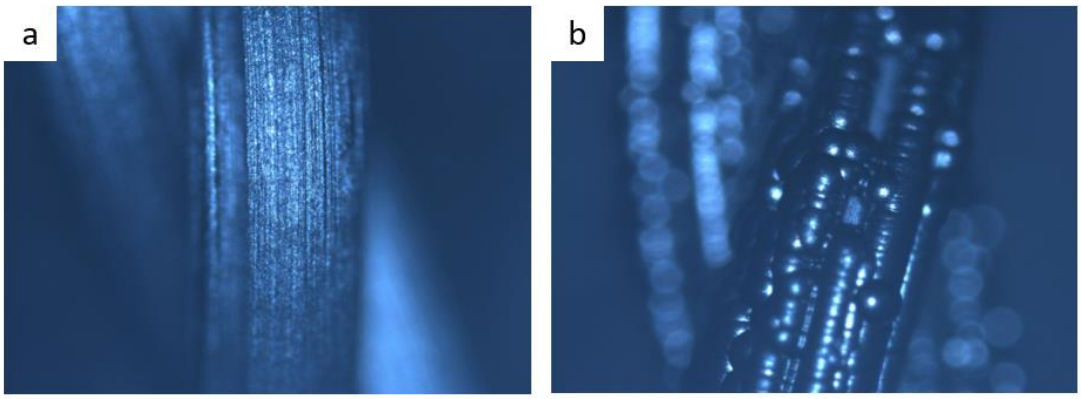

Fig. 23. Optical microscope image of surface of the filaments used in methane concentration of (a) in 1% and (b) in 3%.

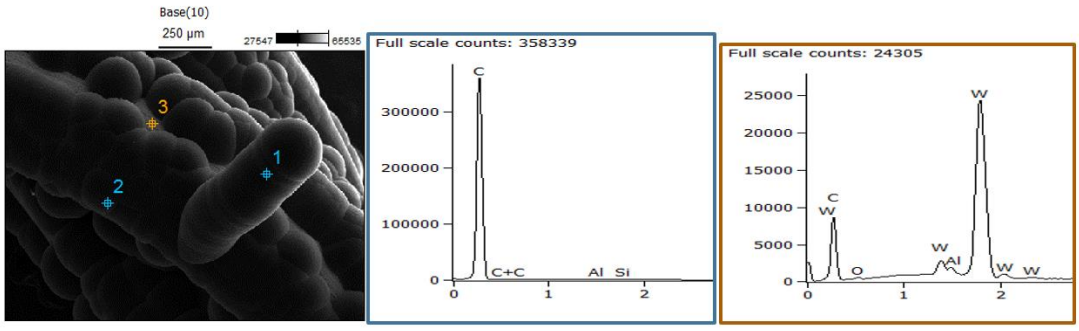

Fig. 24. (left) FESEM image of carbon precipitates on surface of the filament used in 3% methane concentration. (center) EBS data obtained from point#2, which is on one of the carbon precipitates. (right) EDS data obtained from point#3, which is on clean surface of the filament without carbon precipitates.

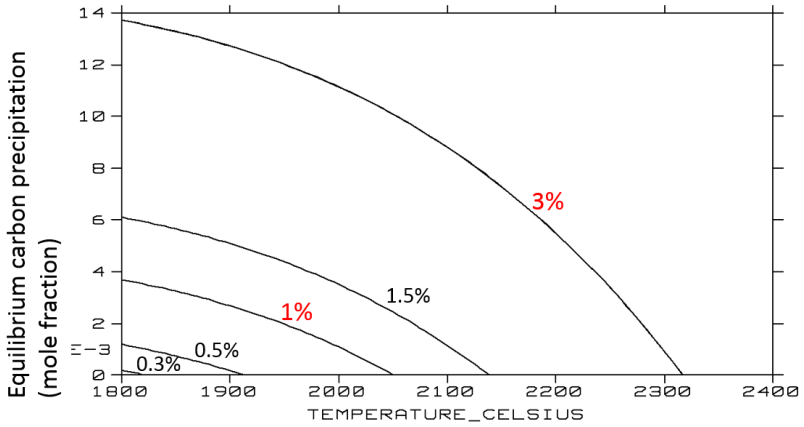

Fig. 25. Thermodynamic calculation of equilibrium carbon precipitation for various carbon concentrations at temperature from 1800 ºC to 2400 ºC using Thermo-calc simulation. X-axis is temperature in Celsius and Y-axis is the equilibrium carbon precipitation in mole fraction.

Difference in the amount of excess charge available for carbon clusters in the gas phase seems to have massive effect on their morphology, and eventually the growth behavior of CVD diamond. It is certain that clusters in the gas phase around the filament at 1900 ºC were fas less charged. Lack of excess charge in nanoclusters lead to formation of non-diamond carbon nanoparticles rather than nanodiamonds, and their coagulation into polycrystalline nanoparticles. Since they were poorly charged, and thus electrostatic repulsion force among nanoparticles was weak, they were observed as coagulated polycrystalline nanoparticles in TEM image.

Morever, difference in surface condition of the filament used in 1% methane concentration and that was used in 3% methane concentration may also have brought huge effect, other than thermionic emission, on charging nanoparticles in the gas phase. The filament used in 3% methane concentration was covered with graphite, which has higher work function value than tungsten carbide. Literature value of work functions of tungsten carbide and graphite are 3.73eV and 4.84eV, respectively. Work function value affects not only thermionic emission of the filament but also the extent of surface ionization.

The amount of current generated by thermionic emission is given by Richardson's law of thermionic emission.

$$\mathrm{J} = A_G T^2 e^{-\frac{W}{kT}}$$

where J is the emission current density, T is the temperature of metal in Kelvin, W is the work function of the metal, k is he Boltzmann constant, A_G is a constant related to material-specific correction factor. Certainly, graphite coating on the tungsten filament reduces its thermionic emission, by reducing exposed area of tungsten filament, and by binding electrons with higher work function value than that of tungsten carbide.

Moreover, graphite coating on the filament impedes surface ionization of carbon molecules in the gas phase, which occurs when these molecules directly collide on surface of the hot filament. The relationship between surface ionization and work function value of the surface materials is given by Saha-Langmuir equation.

$$\frac{n_+}{n_0} = \frac{g_+}{g_0} e^{-\frac{W-V}{kT}}$$

Where $\frac{n_+}{n_0}$ is the fraction of ionized molecules, $\frac{g_+}{g_0}$ is the fraction of statistical weights of the ionic and atomic states, W is the work function of the filament, V is the ionization energy of the element, k is the Boltzmann constant and T is the temperature of surface in Kelvin. The equation has various forms, but it can be interpreted that energy barrier for transferring electron between a molecule and a material is lowered when the molecule has great ionization energy or electron affinity. Among various carbon compounds existing in the gas phase in HFCVD system, C_2 molecule is known for its large

lectron affinity: 3.6eV. Comparison of C_2 molecules' probability of being negatively charged upon collision on surface of tungsten carbide and that of graphite shows that it is a thousand times more probable for C_2 molecules to be negatively charged upon collision with tungsten carbide. C_2 molecules are known as common element generated when methane is decomposed in HFCVD system. Therefore, they can largely contribute in making nanodiamonds with excess negative charge in the gas phase.

All things considered, we can conclude that nanoparticles existing in the gas phase are more negatively charged in 1% methane concentration than in 3% methane concentration, and when the filament temperature is above 2000 ºC than when filament temperature is below 2000 ºC. Moreover, as filament temperature decreases in 3% methane concentration, massive change in morphology of nanoparticles has been observed. Lack of excess charge in the carbon clusters in the gas phase lead to formation of non-diamond carbon clusters, and polycrystalline clusters.

Since the deposition condition of CVD diamond is well known to be etching environment for graphite, these non-diamond carbon clusters are likely to be etched away, too. Diamond is also under etching condition, but its solid crystal structure makes the etching process very slow and therefore does not affect. Enventually, only diamond nanoparticles existing in the gas phase are able to contribute to the formation of CVD diamond. Other non-diamond carbon clusters are etched away before reaching the substrate and do not contribute to the growth of diamond film. That is why the growth rate of diamond film is inversely proportional to methane concentration when filament temperature is lowered. Whereas the filament temperature did not matter much in low methane concentration, high methane concentration combined with low filament temperature made it hard for carbon clusters to be charged, bringing severe drought of nanodiamonds in the gas phase.

10) CVD Growth trials on ultrasmall metal catalysts / diamond seed layer

To mitigate a risk of only relying on a heterogeneous nucleation of diamond on metal catalysts, the Brown team has expanded the approach to the seeded growth of diamond nanowires by seeding the growth on bulk diamonds such as MCD film or diamond nanoparticles. the Brown team has taken tasks of evaluating a stability of the metal catalysts / MCD seed layer structures under high temperature, hydrogen ambient and of attempting the APCVD growth trials on the gold / MCD seed as a starting platform.

Figure 26 shows properties of the commercially-available, 3-μm-thick MCD film grown by hot-filament CVD on a Si substrate. The MCD film had micron-sized grains [Fig. 26(a)] and exhibited a characteristic Raman shift at 1,332 cm^{-1} [Fig. 26(b)]. It is worthwhile to note that the MCD film still maintained a diamond cubic structure even after the CVD growth at high temperature of 900 ºC with the existence of hydrogen [Fig. 26(c)]. Such results guarantee that the MCD film is not transformed to a graphite phase under the experimental conditions in concern.

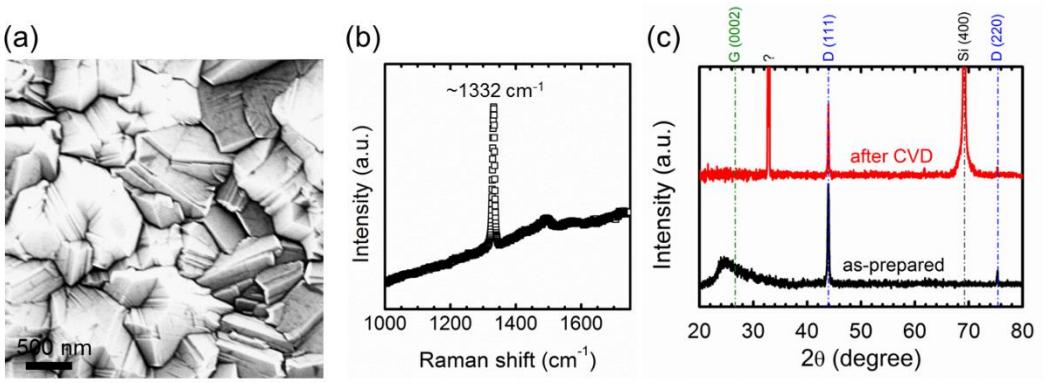

Fig 26. (a) Plan-view SEM micrograph, (b) Raman spectra, and (c) x-ray diffraction patterns of 3-μm-thick MCD films. In (c), "after CVD" denotes the Ni catalysts/MCD sample undergone the actual CVD process at 900 ºC. A question mark in (c) originated from an artifact of the underlying Si substrate.

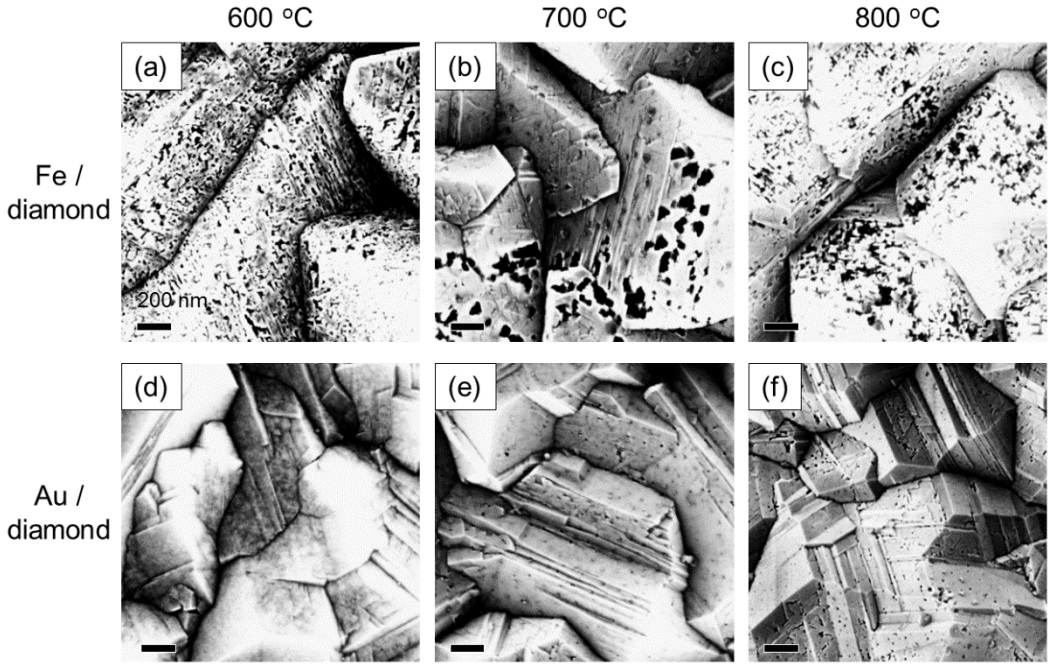

Fig 27. Plan-view SEM micrographs of (a-c) Fe / diamond and (d-f) Au / diamond structures annealed at (a, d) 600, (b, e) 700, and (c, f) 800 °C under hydrogen ambient (pressure: 100 Torr). Initial thicknesses of evaporated Fe and Au catalysts were 1 nm. Scale bar indicates 200 nm.

Once the thermal stability of the MCD films was confirmed, ultrasmall catalysts (Fe, Ni, Co, or Au) were formed on the MCD surface by depositing ultrathin film (~1 nm in thickness) *via* e-gun evaporation and by subsequently agglomeration during heat-up stage. As a testbed, the catalysts / diamond platforms were preliminarily annealed at various temperatures (600 - 950 °C), without flowing carbon precursors (e.g. methane). Unexpectedly, we found the underlying diamond was significantly etched by the metal nanocatalysts if hydrogen was flowed in the chamber. Figure 27 shows (a-c) Fe/diamond or (d-f) Au/diamond structures annealed at 600 - 800 °C under the hydrogen ambient at a pressure of 100 Torr or lower. Regardless of the tested temperatures, the Fe / diamond samples exhibited the catalyst and hydrogen-induced etch phenomena even at a relatively low temperature of 600 °C. Similar etch phenomena were also observed in previous publications by Mehedi *et al.* and Ohashi *et al.* [H.-A. Mehedi *et al.*, *Nanotechnology*, 23, 455302 (2012). / T. Ohashi *et al.*, *Diamond Relat. Mater.*, 20, 1165 (2011).] Such etch phenomena also affected the actual CVD process with flowing methane as carbon precursors and limited a process window greatly. It is suggested that carbon atoms in the diamond substrate were dissolved into the metal nanoparticles with high carbon solubility at high temperatures and, once carbon atoms are supersaturated, those atoms react with hydrogen and are released by forming methane or any other hydrocarbon gas species. Indeed, our experiments revealed that the use of gold or copper, with much lower or no carbon solubility (0.07 at% for Au at 1,000 °C, 0 at% for Cu), significantly retarded the etch process and no etch observed at all at 600 °C or below [Fig. 27(d-f)]. In addition, we also found that, if the CVD growth was made at atmospheric pressure, this metal-induced etch of diamond was minimized, probably owing to much higher deposition rate compared to its etch rate of the diamond substrate.

Based on these preliminary observations, the Brown team has started the efforts on APCVD growth of diamond nanowires using ultrasmall gold catalysts (1-nm in initial thickness) / MCD platforms. Gold was chosen as a candidate catalyst since it has low carbon solubility, which is probably beneficial for suppression of the underlying diamond etch, and is known to produce amorphous carbon nanowires [D. Takagi *et al.*, *Nano Lett.*, 8, 832 (2008).] which can be hopefully turned into diamond with existence of the diamond seed as in our platform. Figure 28 shows carbon nanowires grown on Au / diamond structures by APCVD. Those nanowires were grown at 950 °C for 1 hour and flow rate ratios of argon / hydrogen were widely varied to optimized growth parameters, while a methane flow rate was fixed to 150 sccm (30 %). Some of wire morphologies were observed in the optimal conditions [Figure

28(b, c)], while deposition of non-nanowire amorphous carbons on the MCD substrate [Figure 28(a)] or curly nanotubes [Figure 28(d)] were observed if hydrogen was poor or rich. Meanwhile, there were almost negligible growths occurred if the growth temperature was 900 °C or lower.

One of the optimal specimen [in Figure 28(c)] was analyzed byTEM to confirm a phase of nanowires. Figure 29 shows plan-view (a) bright-field and (b, c) high-resolution TEM images of the carbon nanowires grown on the Au / diamond structure. The nanowires were dispersed in ethanol and dropped onto a TEM grid with amorphous carbon / formvar support. The results showed that the nanowires have an amorphous carbon phase. It is suspected that a relatively large lattice mismatch between gold and diamond (~14 %) prohibited epitaxial growth of diamond nanowires. Instead, the team is planning on replacing gold into copper since it has very small lattice mismatch to diamond (only 1.2 %) but still has negligible carbon solubility. Potentially modification of the surface state of the MCD films may exclude a possible existence of the graphite phase on the surface so that to ensure epitaxial growth of diamond nanowires from the MCD films.

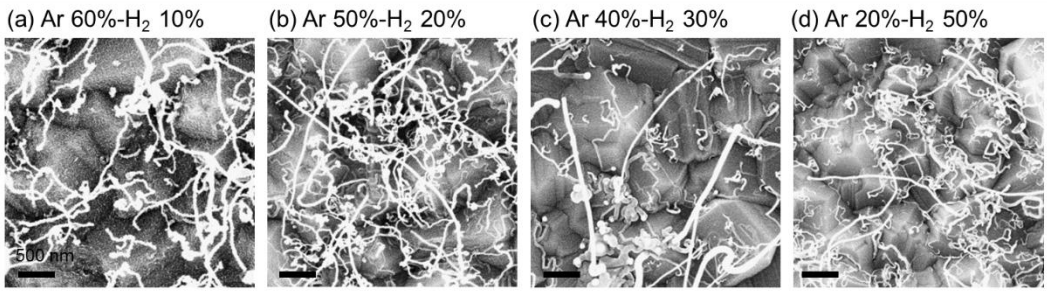

Fig 28. Plan-view SEM images of carbon nanowires grown on Au / diamond substrates by APCVD. The nanowires were grown at 950 °C for 1 hour. Total gas flow rate and a flow rate of methane were fixed to 500 sccm and 150 sccm, respectively, while flow rate ratios of argon and hydrogen were varied. Initial thickness of Au catalyst was 1 nm. Scale bar indicates 500 nm.

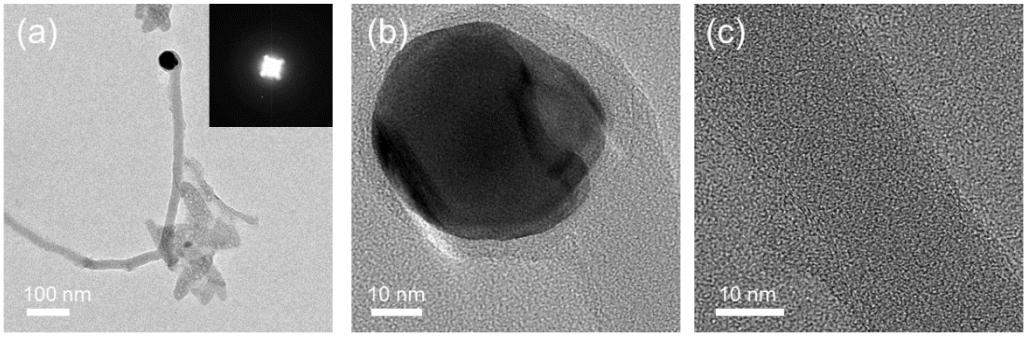

Fig 29. Plan-view (a) bright-field and (b, c) high-resolution TEM images of the carbon nanowires grown on the Au / diamond structure. The nanowires were grown at 950 °C for 1 hour with a gas flow ratio of Ar 200 - H_2 150 - CH_4 150 sccm.

11) Growth trials of crystalline carbon nanowires on graphitic carbon seeds

The Brown team has continued on the seeded growth approaches for reproduction of diamond nanowires. The team has given efforts to avoid the undesirable etching of the diamond seed by introducing source gas (e.g. ethylene, C_2H_4) with low decomposition temperature. Preliminary results were summarized in Fig. 30. Owing to the introduction of C_2H_4 gas, the growth temperature could be much lowered down to 500 -600 °C. However, even at these low temperatures, iron catalysts made tiny holes onto the diamond seed [Fig. 30(a)]. In contrast, nickel seemed to be a better option since there were no etch pits or holes formed at all. The grown nanomaterials were curly as in the case of typical carbon nanotubes. It is suspected that the temperature used in this process (500 - 600 °C) was not enough for catalyzing the formation of sp^3 bonds required for the diamond growth. In Fig. 30(c), copper catalysts resulted in no growth of carbon nanomaterials. This indicates that copper is not suitable as a

catalyst for decomposing carbon sources at low temperature. Gold was also tested but produced the same results with copper. The team will turn direction to modify surface of the microcrystalline diamond to remove any graphitic or non-diamond carbons on the surface by applying low temperature air anneal and/or hydrogen plasma treatment prior to the deposition of metal catalysts / CVD process.

In parallel, the Brown team has tried a new approach on the seeded growth of diamond nanowires. In theory, it was expected that diamond can be epitaxially grown at edges of graphite, as schematically described in Fig. 31(a) [W. R. L. Lambrecht *et al.*, *Nature*, **364**, 607 (1993).]. Specifically, if the (0001) planes of the graphite are aligned to (111) planes of diamonds, it has a possibility of growing diamond nanowires from pre-formed graphitic carbon seeds. Indeed, the Brown team observed the clue. Fig. 30(b) shows the nucleation of diamond on the edge of graphite nanowire during CVD process, as observed at the early stage of the diamond nanowire synthesis [C.-H. Hsu, Ph.D. dissertation in Brown University (2011).]. This clue has inspired us to explore a graphitic carbon as a new seed layer for the diamond nanowire growth.

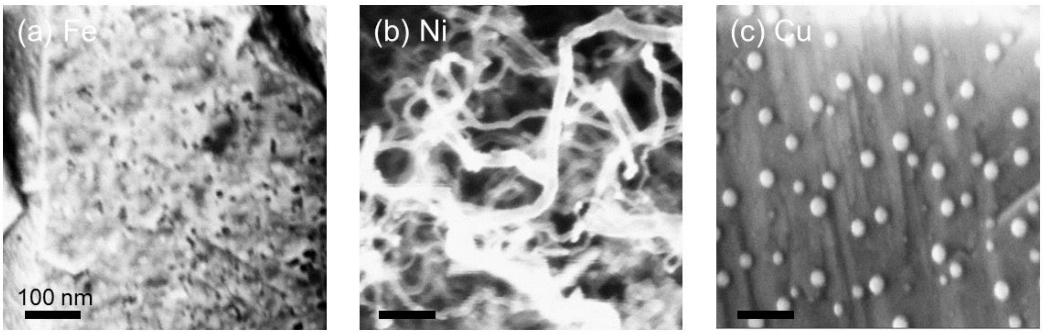

Fig. 30. SEM micrographs of catalysts (Fe, Ni, or Cu) / microcrystalline diamond seed after CVD growth using C_2H_4 as aprecursor. The CVD process was undergone at 600 ^oC, atmospheric pressure for 1 hour with gas flow rates of Ar 300-H_2 100-CH_4 100 sccm. 3-μm-thick industrial microcrystalline film was used as a seed layer.

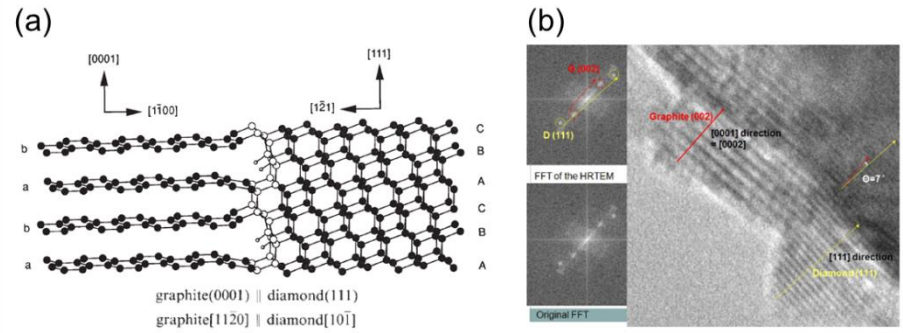

Fig. 31. (a) Epitaxial relationship between graphite and diamond [21]. (b) Chance observation of diamond nucleation at edge of a graphite nanowire during APCVD process [22].

To realize this approach, 5-nm-thick amorphous carbon (*a*-C) was e-gun evaporated on SiO_2/Si wafers, and then ultrathin metal catalyst (1-nm-thick Fe, Ni, or Co) was evaporated atop the *a*-C. Upon heating up to 900 ^oC, this *a*-C layer is expected to be crystallized into graphitic carbon or graphene. With assumption of partial exposure of graphitic edges at the catalyst surface, the epitaxial growth of the diamond nanowires on top of those edges was designed. At the same time, the graphitic carbon can work as a protecting layer to prohibit evaporation of ultrasmall catalysts at high growth temperature.

Among the numerous trials on various iron-family catalysts, Fig. 32 shows the representative growth results on Co / *a*-C structure. Unlike the bare SiO_2 surface which showed no growth, the *a*-C surface provided catalytic effects for growth of both straight nanowires and other carbon species. It's

remarkable that the straight nanowires with a length of 5 μm or longer were grown on the Co / *a*-C structure. These straight carbon nanowires have been observed in a wide range of the process conditions. Fig. 28 shows the nanowires grown at 900 °C with varied methane (CH_4) flow rate from 20 to 60 % with a fixed hydrogen flow rate of 20 %. Such results indicate that this new approach has a wide process window.

One of the concerns or obstacles is that, even in this new seeded growth system, both straight nanowires and curly nanotubes were grown simultaneously. In order to increase a possibility of finding straight nanowires during a post-growth sorting process, post-air anneal has been applied. It was reported that the post-air anneal process can selectively remove sp^2 and other carbon species from nanodiamonds [S. Osswald *et al.*, *J. Am. Chem. Soc.* 128, 11635 (2006).]. The Brown team has given trials on one of the best samples grown on the Co / *a*-C structure. Figure 34 shows SEM micrographs of (a) as-grown and (b-c) post-air annealed samples at 400 and 450 °C, respectively. While the sample annealed at 400 °C was almost intact, the nanomaterials annealed at 450 °C were almost burnt and only straight nanowires were selectively left. Raman spectra (inset) also showed that broad peaks, as characteristics of amorphous carbon, were lifted off after annealed at 450 °C. Beyond the period of this project, the Brown team is continuing on further optimizing the post-air anneal conditions (temperature, time, pressure) to selectively leave the straight and possibly highly crystalline nanowires and to minimize time required for the post-sorting process in a consequent analysis of TEM, SAED, EELS, and Raman of single or multiple nanowires.

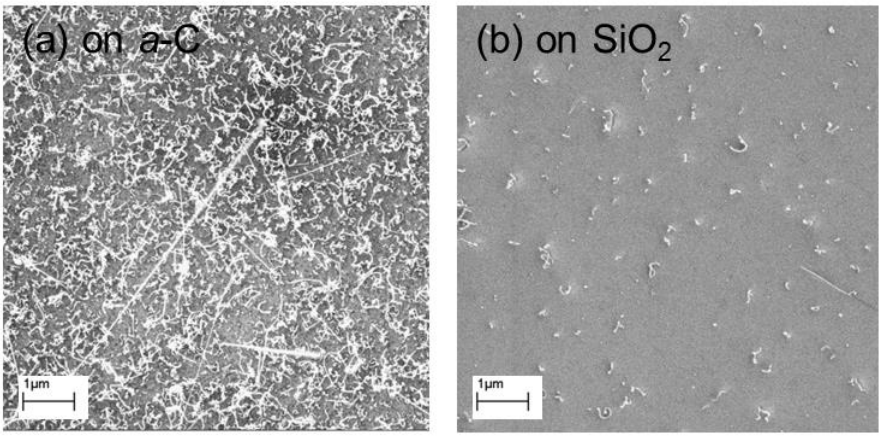

Fig. 32. SEM micrographs of carbon nanomaterials grown on Co catalysts atop the (a) *a*-C and (b) SiO*2* surfaces. The growth was performed at 900 °C, atmospheric pressure for 1 hour with gas flow rates of Ar 400-H_2 100-CH_4 100 sccm.

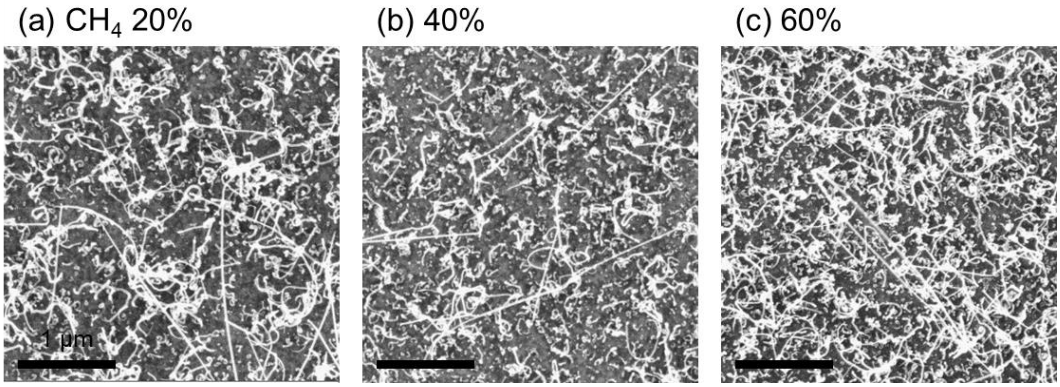

Fig. 33. SEM micrographs of carbon nanomaterials grown on Co / *a*-C structures with methane flow rate ratio of

(a) 20%, (b) 40%, and (c) 60%. The growth was performed at 900 ºC, atmospheric pressure for 1 hour and total gas and hydrogen flow rates were fixed to 500 and 100 sccm, respectively.

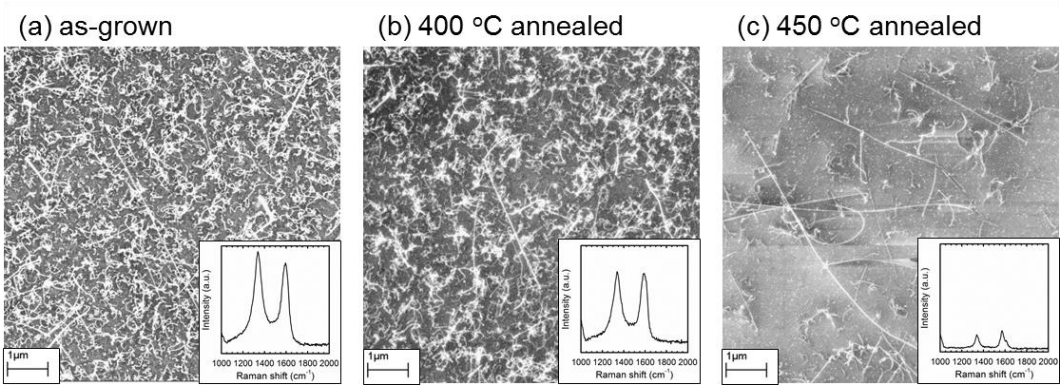

Fig. 34. SEM micrographs of (a) as-grown and (b,c) post-air annealed specimens at (b) 400 ºC and (c) 450 ºC. Inset shows corresponding Raman spectra taken with a incident laser wavelength of 532 nm. The post aneal was conducted in air for 1 hour. Initial growth was made at 900 ºC, atmospheric pressure for 1 hour with gas flow rates of Ar 350-H_2 100-CH_4 50 sccm.

12) Fabrication of porous Si by gas-phase metal-assisted etch process

Unexpected finding of the etch of diamond film by metal catalyst under hydrogen ambient motived the Brown team to explore a new approach of fabricating a porous Si which is to be used for generation of single photon sources. In the previous efforts, Brown team has found a new color center, as named "Si-G centers", by forming periodic holes on a surface of silicon using a reactive ion etch [S. G. Cloutier *et al.*, *Nature Mater.* **4**, 889 (2005)]. This Si-G center consisted of two carbon substitials and one silicon interstitial. At that time only lasing properties of the porous Si has been studied but a potential as a single photon source has not been explored. Thanks to the support of this project, Brown team has explored a new method of fabricating porous Si by a simple gas-phase metal-assisted etch process. Unlike a conventional metal assisted chemical etch (MACE) which is based on wet chemical reaction with a possible electrochemical contamination of the Si surface, this new method, named as metal-assisted gas-phase etching (MAGPE) utilizes the diffusion of underlying Si into nano-gold catalysts and subsequent catalytic reaction of supersaturated Si with hydrogen gas (or atomic hydrogens dissociated catalytically), as schematically described in Figure 35, Thereby this MAGPE can be free of wet-chemical/electrochemical damages, plasma-damages, and is no need of mask or patterning process. During the efforts of this project, Brown team has focused on fabricating porous Si by using this new concept.

Figure 36 shows an example of porous Si formed by using ultrathin gold catalyst (1-nm-thick) under hydrogen ambient at 750 ºC and at 10 Torr. Unlike bare Si surface [w/o catalysts, Fig. 36(a)], the porous surface has been easily formed with the aid of catalysts and hydrogen gas [Fig. 36(b)]. The etch process has been observed dominantly as thinner (i.e. smaller) gold catalyst is used. In addition, temperature and working pressure greatly affected the formation of pores on the Si surface. Figure 37 shows the process window of MAGPE as a function of pressure and temperature where the points denoted with squares or circles indicate the successful formation of pores. When the catalyst was not introduced, the temperature higher than 750 ºC and the pressure lower than 1 Torr was required to make big-sized, rectangular pores [Fig. 36(a)]. In contrast, by adding 1-nm-thick layer of gold on top of the Si, the process window greatly expanded as shown in Figure 37(b). For example, only the temperature of 650 ºC was required when the pressure was 1 Torr. At 750oC, the pressure window has extended even up to 100 Torr. The process developed in this study will be published in a due course of time. The team is now transitioning to realize Si-G centers into this porous Si template by using either ion implantation or plasma treatment with carbon precursor radicals.

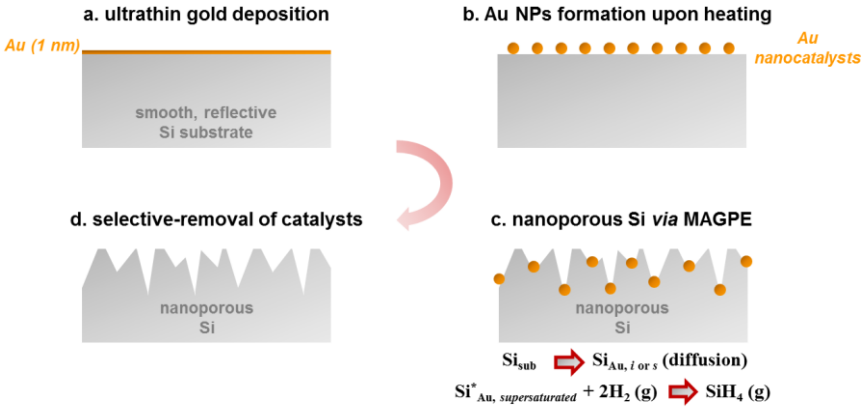

Fig. 35. Schematic process of MAGPE for fabrication of porous Si. Ultrathin gold (1 - 50nm in thickness) was deposited on top of Si surface to initiate formation of pores with aid of hydrogen gases.

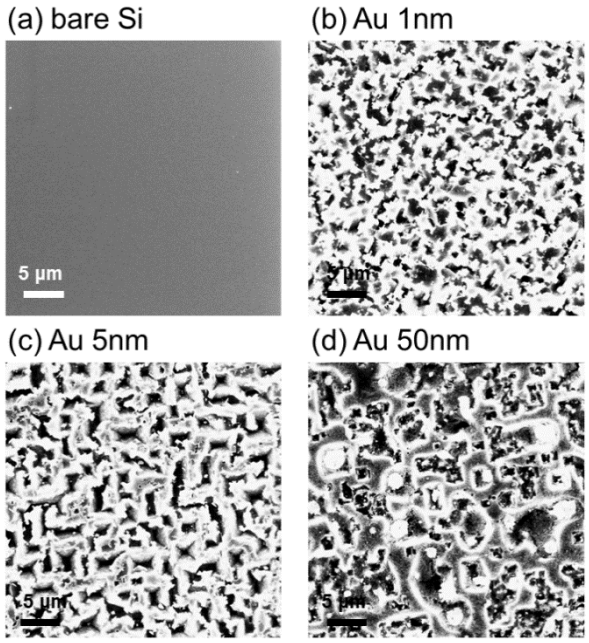

Fig. 36. SEM images of porous Si formed by (b) 1-nm, (c) 5-nm, and (d) 50-nm-thick gold catalysts. (a) bare Si without catalysts had no pores formed. The structures were annealed at 750 °C and at 10 Torr under hydrogen ambient for 1 hour.

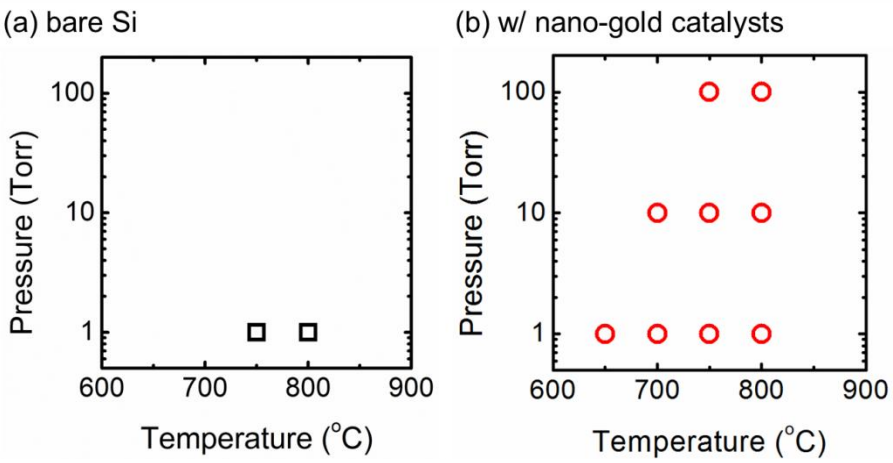

Fig. 37. Process window of MAGPE process as a function of pressure and temperature. Squares or circles indicate the successful formation of pores.

List of Publications and Significant Collaborations that resulted from your AOARD supported project: In standard format showing authors, title, journal, issue, pages, and date, for each category list the followings:

a) Invited Talks

[1] (**Invited talk**) Jimmy Xu, "Diamond Nanowires – Challenges from the Extremes", Fundamental Forum in UESTC, July 22, 2015, China.

[2] (**Invited talk**) Jimmy Xu, "Challenges of the extremes in the pursuit of a new form of carbon nanostructure - Diamond Nanowires", 2016 NSF-AFOSR-ARO-DTRA Workshop on Reproducible Advanced Technologies for Next-Generation Nano/Quantum Devices, April 27-28, 2015, USA.

[3] D.-J. Lee, J.-Y. Kwon, J. Kim, K.-J. Kim, Y.-H. Cho, S.-Y. Cho, S.-H. Kim, J. Xu, and K.-B. Kim, "Atomic Layer Deposition of Amorphous In-Zn-O Films: A New Route to Ultra-Smooth and High Electron Mobility Transparent Conductors", 15th International Conference on Atomic Layer Deposition (ALD 2015), July, 2015, Portland, USA.

[4] D.-J. Lee, J. Kim, G. E. Fernandes, J. H. Kim, C. M. Bledt, S.-Y. Cho, K.-B. Kim, and J. Xu, "Atomic-Layer Doping Induced Transparency Enhancement and Bandgap Widening Beyond the Burstein-Moss Effect", 15th International Conference on Atomic Layer Deposition (ALD 2015), July, 2015, Portland, USA. (Honored "Best Poster Presentation Honorable Mention")

[5] Nong-Moon Hwang, "Non-classical Crystallization of Thin Films and Nanostructures", 2nd Annual World Congress of Smart Materials-2016, Grand Copthorne Waterfront Hotel, Singapore, March 4-6, 2016.

[6] Nong-Moon Hwang, "Non-classical crystallization of thin films and nanostructures synthesized by chemical vapor deposition", THERMEC'2016, Graz, Austria, May29 – June 3, 2016.

[7] Nong-Moon Hwang, "Non-classical crystallization in the growth of diamond and silicon films in the HWCVD process", Hot Wire Chemical Vapor Deposition 9, Chemical Heritage Foundation, Philadelphia, PA, USA, September 6 – 9, 2016.

[8] Nong-Moon Hwang, "Role of Charged Nanoparticles in the Growth of Thin Films and Nanostructures in Plasma and Non-Plasma CVD" 77th Japan Society of Applied Physics Autumn Meeting, Toki Messi, Niigata, Japan, Sept. 13 – 16, 2016.
[9] Nong-Moon Hwang, "Role of Charges in Non-Classical Crystallization of Thin Films and Nanostructures in the Plasma CVD Process", Electrochemical Society, Pacific Rim Meeting on Electrochemistry (ECS PRiME) Honolulu, HI, USA, Oct. 2-7, 2016.

[10] (**Invited talk**) Nong-moon Hwang, "Syntheses of Nanoparticles and Nanowires Using Charged Nanoparticles Spontaneously Generated in the Gas Phase during Chemical Vapor Deposition", 2017 MRS Spring Meeting & Exhibit, April 17, 2017, USA

[11] Jimmy Xu, "A pursuit of extremes in materials science", 4th Aerospace Engineering and Advanced Functional Materials conference, Xiangtan, China Oct 10-11, 2016.

[12] Jimmy Xu, "Frontier Carbon Photonics – single photon sources and detection", 2016 China International Carbon Materials Conference, Shanghai, China, Dec 8-9, 2016.

[13] Z.J. Liu and Jimmy Xu, "Amplifications strategies for graphene infrared detection", SPIE AOPC 2017, Applied Optics and Photonics China 2017, Beijing, June 4-6, 2017.

[14] Jimmy Xu, "Honor and Dream – Failure and Hope", Special Forum for Junior Faculty Members, UESTC Optoelectronics Institute, China, June 8, 2017.

[15] H.-Y. Kim, B.-K. Song, K.-S. Kim, and N.-M. Hwnag "Preparation of Diamond Nanoparticles for Single Photon Emission", The 4th international Symposium on Hybrid Materials and Processing (HyMaP 2017), November 5-8, 2017, Haeundae Grand Hotel, Busan, Korea

[16] H.-Y. Kim, B.-K. Song, K.-S. Kim, and N.-M. Hwnag "Preparation of Diamond Nanoparticles for Single Photon Emission", The 11th Aisoan-European International Conference on Plasma Surface Engineering, September 11-15, 2017, Lotte Hotel, Jung-mun, Jeju Island, Korea

[17] H.-Y. Kim, B.-K. Song, K.-S. Kim, and N.-M. Hwnag "Preparation of Diamond Nanoparticles for Single Photon Emission", Advanced Materials World Congress(AMWC), February 4-8, 2018, Royal Caribbean Cruise, Singapore

[18] H.-Y. Kim, B.-K. Song, K.-S. Kim, and N.-M. Hwnag "Preparation of Diamond Nanoparticles for Single Photon Emission", Hot-Wire Chemical Vapor Deposition 10(HWCVD10), September 3-6, 2018, Kitakyushu International Conference Center, Japan

b) papers published in peer-reviewed journals

[1]. J.-W. Park, N.-M. Hwang, "Gas phase generation of diamond nanoparticles in the hot filament chemical vapor deposition reactor", Carbon, 106 (2016).

[2]. A Badzian, N.-M. Hwang, "Diamond: Low-Pressure Synthesis", *Reference Module in Materials Science and Materials Engineering*, Elsevier, 2016.

[3]. J.-W. Park, K.-H. Kim, N.-M. Hwang, "Non-classical crystallization of diamond deposition in the effect of the substrate bias during hot wire chemical vapor deposition", submitted to Thin Solid Films.

[4]. J.-W. Park, Kwang-Ho Kim, N.-M. Hwang, "Effect of the substrate bias in diamond deposition during hot filament chemical vapor deposition: approach by non-classical crystallization", Advanced Materials Letters, Vol 9 (2018)

c) provide a list any interactions with industry or with Air Force Research Laboratory scientists or significant collaborations that resulted from this work

[1] Brown University visit by SNU team (PI Professor Nong-Moon Hwang and Dr. Jin-Woo Park) and conference call with the group of Michael Check and Luke Bissell, led by Gail Brown, at the Wright-Patterson Base of AFRL (May 16-20, 2016).

d) Other accomplishments

Honors

[1] Chang-Jiang Chair Professorship (visiting), 2015-16, Optoelectronics School, UESTC, China (A program similar to the WCU program of Korea. It comes with a research funding of $50K/yr plus travel support for 3 years, starting from 2014. But the research funds have to stay within the university UESTC, also modeled after the WCU program of Korea.)

[2] Professeur Invite', 2015-16, CNRS-Institut d'électronique de microélectronique et de nanotechnologie and Universite de Lille, France. (An honorary professorship appointment for establishing France-USA collaborative researches on quantum optics and nano-devices. It covers travel and living expenses, ~10K Euro per year).

Contributed talks

[1] D.-J, Lee C. M. Bledt, Y.-H. Cho, K.-B. Kim, and J. Xu, "Counterintuitive Optical Properties of Infrared-Plasmonic Oxide Superlattices by Atomic Layer Deposition", 2017 Materials Research Society (MRS) Spring Meeting, April 17-21, 2017, Arizona.

Awards

[1] Dr. Do-Joong Lee was awarded for "Best Poster Presentation Honorable Mention" by the organizer of the 15th International Conference on Atomic Layer Deposition (ALD 2015) (July 2015).

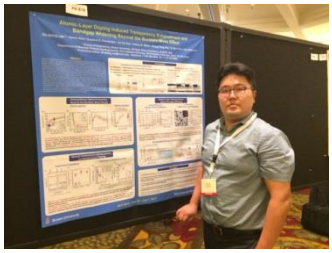

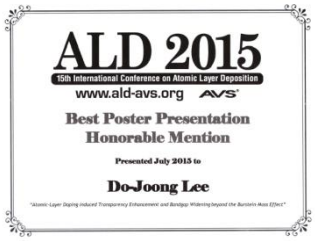

Publication of books

[1] Serge Luryi, Jimmy Xu, Alexander Zaslavsky, ed. "Future Trends in Microelectronics – Journey into the unknowns", Wiley, 2016.

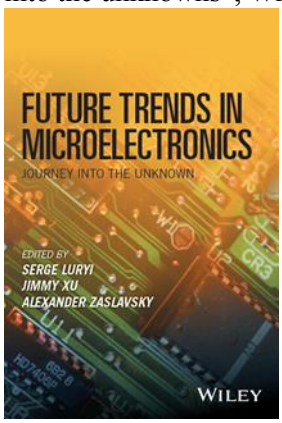

[2]. N.-M. Hwang, *Non-Classical Crystallization of Thin Films and Nanostructures in CVD and PVD Process*, Springer, 2016.